LOST IN TRANSLATION: AN INSIDE LOOK AT TRANSLATION REGULATION OF TOBACCO ETCH VIRUS RNA

by

HASAN YUMAK

A dissertation submitted to the Graduate Faculty in Chemistry in partial fulfillment of the requirements for the degree of Doctor of Philosophy,

The City University of New York

2008

This manuscript has been read and accepted for the
Graduate Faculty in Chemistry in satisfaction of the
dissertation requirement for the degree of Doctor of Philosophy.

Prof. Dixie J. Goss

Date **Chair of Examining Committee**

Prof. Mahesh K. Lakshman

Date **Executive Officer**

Prof. Ruth Stark

Date

Prof. Yujia Xu

Date **Supervisory Committee**

THE CITY UNIVERSITY OF NEW YORK

For Sumeyra and Ihsan

Abstract

LOST IN TRANSLATION: AN INSIDE LOOK AT TRANSLATION REGULATION OF TOBACCO ETCH VIRUS RNA

by

Hasan Yumak

Adviser: Professor Dixie J. Goss

Zeenko and Gallie (2005, J.B.C; 280, 26813-26824) showed that the pseudoknot (PK1) of tobacco etch virus (TEV) RNA is necessary to promote cap-independent translation. We showed the first quantitative data (24) on the binding interactions of plant protein synthesis initiation factors with IRES and demonstrated that the TEV leader can discriminate between eIF4G isoforms to preferentially recruit one isoform over the other. We studied the effect of Poly(A)-binding protein (PABP) on the PK1 RNA binding to eIF4F in the presence and absence of eIF4B. Equilibrium studies of PK1 RNA binding to eIF4F showed ~ 2-fold stronger affinity in the presence of eIF4B. Addition of eIF4B and PABP to the eIF4F enhances binding affinity ~ 4-fold as compared to eIF4F binding to PK1 RNA. Further, we investigated the effect of $Poly(A)_{20}$ on the binding of initiation factors to PK1 RNA. In the presence of $Poly(A)_{20,}$ eIF4F·PABP bound to PK1 about 4-fold tighter. Further, addition of Poly $(A)_{20}$ enhances the binding affinity of eIF4FeIF4B·PABP protein complex by about 3 -fold for PK1 RNA. Overall, eIF4F·eIF4B·PABP·$Poly(A)_{20}$ complex has 11-fold higher affinity to PK1 RNA as compared with binding affinity of eIF4F alone. Kinetic analysis of eIF4F and eIF4F·4B with PK1 RNA were also measured and compared. The stopped-flow fluorescence anisotropy measurements

demonstrated that the observed rate constant for the binding of PK1 RNA increased linearly with an increase in eIF4F and eIF4F·4B initiation factor concentration. The association rate constant (k_{on}) for PK1 binding was ~ 2-fold faster for eIF4F·4B than for eIF4F alone. eIF4F-PK1 RNA complex shows a slower rate of dissociation in the presence of eIF4B (k_{off} = 10.2 ± 0.7 s^{-1} for eIF4F·4B; k_{off} = 11.6 ± 0.3 s^{-1} for eIF4F). Since viral protein synthesis is simpler than host cell protein synthesis, the information obtained from this research has potential use to develop systems to produce desired proteins which are nutritionally beneficial and have other economic uses.

Acknowledgments

My utmost gratitude goes to my thesis advisor, Professor Dixie J. Goss for allowing me to join her team, for her expertise, kindness, and most of all, for her patience. Her wide knowledge and her logical way of thinking have been of great value for me. Her understanding, encouraging, and personal guidance have provided a good basis for the present thesis. I am deeply indebted to her.

I would like to thank Professor Klaus Grohmann for giving me the opportunity to carry out my PhD study at the Department of Chemistry. He was always there whenever I needed help. He was generous with his comments and his advice.

I would like to thank Professor John Trujillo who is a precious member of our lab during summer times. He provided assistance in numerous ways and made it a pleasure to come to the lab.

I would like to thank my committee members, Professor Ruth E. Stark and Professor Yujia Xu, for their time, insight, and comments throughout this experience.

I would like to gratefully acknowledge the support of Dr. Mateen Khan. He helped me immensely by giving me encouragement and friendship. I would not be performing this work without his continual encouragement and support. I was very lucky to have such a good friend and partner at work.

Warm thanks also go to previous and the current members of the lab: Dr. Sibnath Ray, Dr. Diana Friedland, Shemaila Sultana, Artem Domashevskiy, Jia Ma,

Anamika Banarjee, and Brian Hu for creating splendid and humoristic working environment.

Special thanks go to my best friend and closest colleague in the group, Ozgur Ecevit, for helping me get through the difficult times, and for all the emotional support, entertainment, and caring he provided.

Through my study, I always have received the mental and emotional support from my dear family. I thank to my mother, my father, and my brother from my heart for their love and support.

My deepest thanks go to my dear wife and a colleague, Sumeyra, for her love and understanding through my graduate years. She was always behind me and gave her unconditional support even if that meant sacrificing for her time and study. Without her sacrifices and support, I would not have been able to complete my Ph.D. Finally, thanks to our son, Ihsan, for the joy and the happiness he brings to me during our many moments together. With love and gratitude, I dedicate this thesis to my wife and son.

TABLE OF CONTENTS

LIST OF TABLES

LIST OF FIGURES

LIST OF ABBREVIATIONS

elF: Eukaryotic Initiation Factor

TEV: Tobacco Etch Virus

EMCV: Encephalomyocarditis Virus

IRES: Internal Ribosome Entry Site

NATA: N-acetyltryptophanamide

nt: Nucleotide

LB: Luria-Bertani Broth

IPTG: Isopropyl β-D-1-thiogalactopyranoside

HEPES: 4-(2-hydroxyethyl)-1-piperazineethanesulfonic acid

PMSF: Phenylmethanesulphonylfluoride

DTT: Dithiothreitol

SDS-PAGE: Sodium Dodecyl Sulfate Polyacrylamide Gel Electrophoresis

k_{on}: Rate of association constant

k_{off} : Rate of dissociation constant

1.0 Introduction

Translation is reading of a messenger RNA sequence into the amino acid sequence of a polypeptide. It occurs in ribosomes and takes place in three stages; initiation, elongation, and termination. The initiation stage is a complex process in which the Met-tRNAi initiator, 40S, and 60S ribosomal subunits are assembled by eukaryotic initiation factors (eIFs) into an 80S ribosome at the start codon of an mRNA. During elongation, the actual polypeptide synthesis occurs. Termination takes place when the ribosome reaches the stop codon that causes dissociation of completed polypeptide and the ribosome from the mRNA (1-4).

Initiation is the most complex of these stages and is the focus of the many regulatory processes. Translation initiation consists of several steps and is catalyzed by eukaryotic initiation factors, proteins used in eukaryotic translation. Translation initiation requires participation of at least eleven initiation factors. Initiation normally is the rate-limiting step. Contingent on how the 40S ribosomal subunit is recruited, translation initiation can follow either a cap-dependent or a cap-independent mechanism.

1.1 Cap-Dependent Translation Initiation

Virtually all eukaryotic mRNAs possess a 5'-cap structure (m^7G(5')ppp(5')N) that, during translation initiation, functions as the binding site for the eukaryotic initiation factor eIF4E. The cap structure integrates various important functions and affects RNA splicing, transport, stabilization, and translation. In a cap-dependent translation, the cap structure serves as a molecular tag that marks the specific location where the 40S ribosomal subunit is to be recruited.

Cap-dependent initiation is the most common translation initiation mechanism in eukaryotes. In this initiation pathway, the first step is binding of eIF4E, small subunit of eIF4F, to the cap structure. Stimulated by eIF4B, eIF4A unwinds secondary structure in the five prime untranslated region (5' UTR). The interaction of the poly(A)-binding protein, PABP, with eIF4G is proposed to cause circularization of the mRNA. After that, the 40S ribosomal subunit forms a complex with initiation factors eIF2, eIF3, and methionyl-initiator-$tRNA_{Met}$ is recruited to the mRNA. Then, this 43S complex scans the mRNA in a 5' to 3' direction and finds the AUG start codon that causes to the release of eIF2 and eIF3 and binding of 60S ribosomal subunit. The complete 80S ribosome is now competent for translation elongation.

Efficient translation is believed to take place in a closed loop format (Figure 1), in which 5'and 3' termini are brought together into close proximity through the interactions of translation initiation factors (5,6,7).

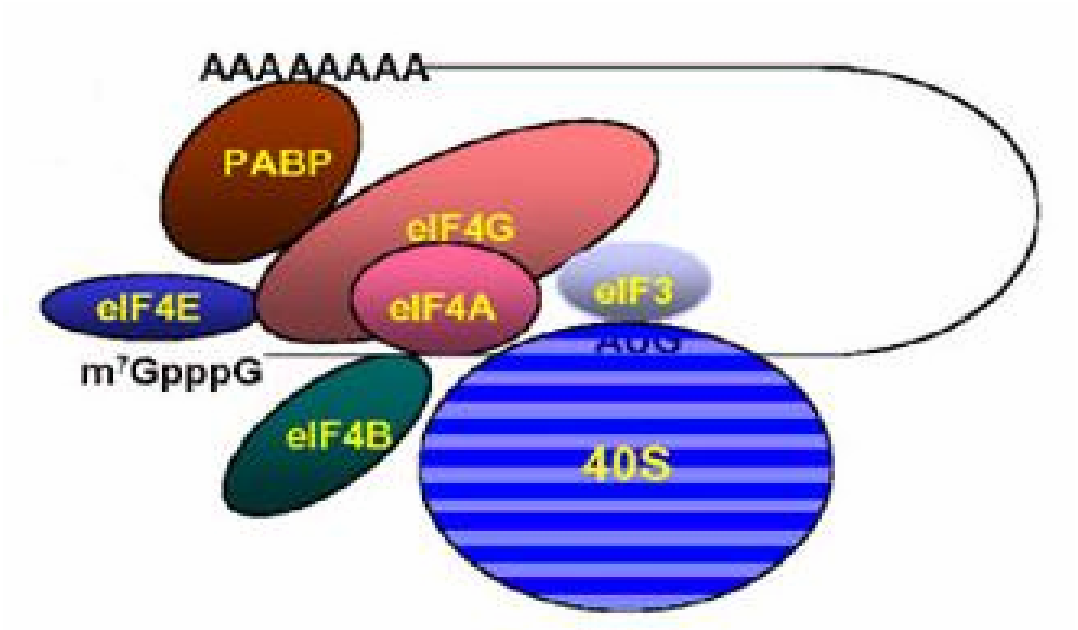

Figure 1. Schematic depiction of the closed-loop model of translation initiation. The eIF4F complex interacts with both the 5'end of the mRNA through eIF4E and the poly(A) tail through PABP and recruits the 40S ribosomal subunit by means of its interaction with eIF3.

1.2 Cap-Independent Translation Initiation

In 1988, it was discovered that translation of the uncapped picornaviral mRNA is mediated by binding of the ribosome to internal ribosome entry site (IRES) elements, RNA structures which enable assembly of the translational machinery at a position close to or directly at the initiation codon (8,9). After that, it was revealed that initiation on several viral and cellular mRNAs is cap-independent. This discovery broke one of the fundamental beliefs of translation initiation, that is, that eukaryotic ribosomes can bind to mRNA only at the 5' end. Animal picornaviruses, such as poliovirus and encephalomyocarditis virus (EMCV), and the plant virus, tobacco etch virus (TEV) are among the viruses that lack a 5' cap structure. Even though IRESs of animal picornaviruses possess long structured noncoding 5' sequence, IRESs characterized from plant viruses are shorter and less structured than those of animal picornaviruses, implying that plant viruses such as TEV are a simpler system with fewer interactions.

The features of typical IRES are not precisely defined. Generally, there are no consequential similarities between individual IRESs. IRESs possess very structured 5' non-translated regions that hinder scanning of ribosomes. Because of the fact that cap recognition is not mandatory in IRES-mediated translation, certain eIFs may not be necessary for initiation (10). In IRESs, small mutations or even substitution of a single nucleotide can cause loss of their function or

enhance their activity (11-15). Thus, the activity of IRES relies on its structural integrity.

It has been shown that most cellular IRESs function preferentially when cap-dependent translation is physiologically impaired. For example, when cells undergo a variety of stress conditions, such as hypoxia, amino acid starvation, irradiation and apoptosis, cap dependent translation is impaired. However, IRES elements were found to be active under these conditions (16-18)

1.3 Tobacco etch virus (TEV)

Tobacco etch virus (TEV) is a plant virus and a member of the picornavirus supergroup of positive strand RNA. The genomic RNA of TEV is polyadenylated and in the 143-nt 5'-leader sequence an IRES site that provides efficient translation of the RNA is found. The 5'-leader of TEV folds into a structure consisting of two domains, each of which possesses RNA pseudoknots. Mutational studies (19) showed that the first pseudoknot (PK1) that contains a nucleotide sequence complementary to a highly conserved region of 18 S rRNA is important for IRES activity. PK1 (49bp) is an H-type pseudoknot with two stems, S1 (6 bp) and S2 (5 bp) that are linked by loops L1, L2, and L3. S1 and S2 stems are separated by 2nt of L2 (Figure 2).

The full-length TEV leader has more single stranded regions than does PK1. Mutation in the loop 3 region of PK1 so called S1-3, which damages its potential base pairing with 18SrRNA, decreased translation to ~ 7.4 % of wild type levels (19). It has been shown that the poly(A) tail and the TEV 5'-leader functionally interacts to aid cap-independent translation (20-22)

Employing wheat germ lysate depleted of eIF4F/eIFiso4F (23) has revealed that eIF4F is essential for cap independent translation. Supplementation of eIF4F into the depleted lysate enhanced expression of TEV. Accordingly, the addition of eIF4F decreased the translational advantage conferred by the TEV IRES from a level of a 167-fold enhancement of

translation to merely 14-fold enhancement while addition of eIFiso4F did not reduce the translation of TEV IRES. These results showed that eIF4F alone is adequate for the translation of TEV IRES. In addition, quantitative binding affinity studies from our lab (24) demonstrated that PK1 favorably binds with eIF4F rather than eIFiso4F.

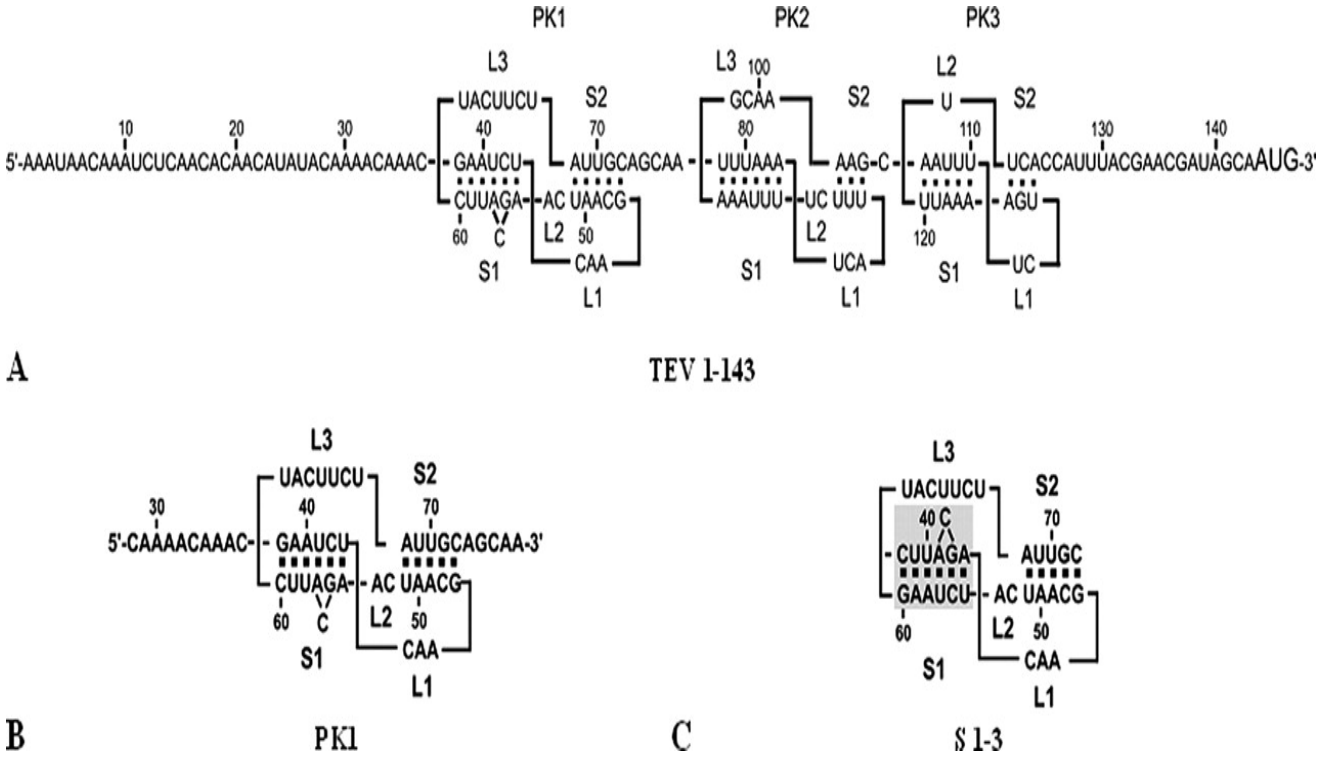

Gallie et al 2005

Figure 2. The predicted structure of TEV 5'-leader. A, the entire TEV 5'-leader (nt 1-143); B, the pseudo knot PK1 (bases: 28-77) of TEV 5'-leader; C, Mutation of Stem 1-3 of pseudo knot PK1.

1.4 eIF4F

Wheat germ and other plants express two related but distinct forms of the cap binding complex designated as eIF4F and eIFiso4F (25). Both proteins consist of two subunits, eIF4E (molecular mass 26 kDa) and eIF4G (molecular mass 165 kDa), and eIFiso4E (molecular mass 28 kDa) and eIFiso4G (molecular mass 86 kDa). eIF4F and eIFiso4F have a number of functional similarities. They serve in supporting cap-dependent in vitro translation, facilitate ATP-dependent helicase activity, and function as RNA-dependent ATPase (25-29). Wheat germ eIFiso4F can substitute for mammalian eIF4F in cross-linking of mammalian eIF4A to the cap of oxidized mRNA and in RNA-dependent ATPase activity (30). Binding studies with oligonucleotides showed that both eIF4F and eIFiso4F recognize the m7G cap structure but differ in the recognition of other structural features suggesting that eIF4F binding is sensitive to the presence of secondary structures and that eIFiso4F demonstrates a binding preference for linear structures (31). It was found that eIF4F supports translation of RNA accommodating secondary structure in the noncoding region better than did eIFiso4F (32). Further studies revealed that in vitro translation using the tobacco etch virus 5′ leader, that naturally lacks a cap, to direct cap-independent translation specifically depended on eIF4G and not eIFiso4G (33). eIF4G works as an adapter protein bringing together mRNA, eIF4E, and eIF4A for binding to the 43S pre-initiation complex. It has been shown that eIF4F interacts with PABP to enhance its RNA binding activity and interaction

between PABP and eIFiso4F increases the binding affinity of cap analogs by about 40-fold (7).

1.5 eIF4B

Mammalian eIF4B stimulates the ATPase and RNA helicase activity of eIF4A and enhances the ATP affinity of eIF4A while wheat eIF4B shows slight stimulation on ATPase and RNA helicase activity of eIF4A (34-40). Previously it was shown that wheat germ eIF4B lowers the activation energy of both eIFiso4F and the eIFiso4F-PABP complex for binding to the 5' cap, implying that eIF4B and PABP improve binding by maintaining a lower energy barrier that may entail a conformational change, propagated to the cap binding site (41,42). Moreover, eIF4B mediates mRNA binding to ribosomes (43-45). The interaction of eIF4G or eIFiso4G and eIF4B with PABP enhances the binding affinity of PABP for poly(A) tail (46). Hence, eIF4B has multiple roles through interactions with several factors and RNA to facilitate translation initiation. It stabilizes eIF4F binding to the 5' cap, PABP binding to the poly(A) tail, and mRNA binding to ribosomes. This shows that eIF4B carries out various functions through interactions with several factors and RNA to promote translation initiation.

Wheat eIF4B was demonstrated to bind poly (G) and poly(A) RNA (47). This showed that in addition to the animal and yeast eIF4B, plant eIF4B is

an RNA-binding protein. (48). Further studies (40) showed that wheat eIF4B contains three RNA binding domains. Mammalian and yeast eIF4B have two RNA binding domains. Plant eIF4B contains a novel N-terminal RNA binding domain that requires a short, lysine-rich containing sequence.

There is a limited conservation between wheat eIF4B and other species. For example, eIF4B from wheat shares 29 and 24% identity with eIF4B from human and from Saccharomyces cerevisiae, respectively (48). This makes eIF4B one of the least conserved of the translation initiation factors.

1.6 Poly(A) Binding Protein (PABP)

It has been demonstrated that Poly(A) binding protein, PABP, is essential for 40S ribosomal subunits binding to a mRNA and for formation of the 48S initiation complex (49,50). During initiation of translation, PABP binds eIF4G, therefore facilitating recruitment of the 40S subunit. However, it also has been shown that PABP can stimulate translation independently of its interaction with eIF4G and poly (A) by an undetermined mechanism (51). While PABP binds exclusively to poly (A), it shows lower affinity for poly (U) and poly (G) and no measurable binding to poly (C) (52-55). Using mobility shift analysis, it has been examined whether the association of eIF4F, eIF(iso)4F, eIF4B and eIF4A with PABP have an effect on PABP RNA activity. The results showed that eIF4F, eIF(iso)4F, and eIF4B interact individually with PABP to enhance its RNA binding activity. eIF4A did not cause any significant

increase of PABP RNA binding activity (7). Further, association of eIF4F (or eIF(iso)4F) and eIF4B has a better stimulatory effect on PABP RNA activity than do these initiation factors when present individually with PABP. In addition, cap binding to eIF4F (or eIF(iso)4F) increases binding affinity of eIF4F for PABP by about 40 fold (50). Similarly, interaction between PABP and eIFiso4F has been reported to enhance the binding affinity of cap analogs by about 40-fold (50). An interaction of PABP with eIF4G is conserved among yeast, animals, and plants (7, 49) and stabilizes the binding of eIF4F to the 5'-cap (50). The interaction between PABP and eIF4G or eIF4B enhances the PABP RNA binding activity to poly(A) by 2-fold (50,7) . This shows that that the physical interaction between all three proteins aids in stabilizing their association with their respective binding sites to increase their function during initiation of translation.

1.7 The 3' Poly (A) Tail

Most eukaryotic mRNAs possess a poly (A) tail that is added to the 3' -end of the pre-mRNA by translation initiation complex. It has been proposed that poly (A) tail affects every aspect of mRNA processing and metabolism. For instance, it has been suggested to take a role in conferring RNA stability and enhancing translation efficiency. It has been shown that 3' poly(A) of mRNA promotes translation even in the absence of a 5'-terminal m^7G cap and acts synergistically with the cap to increase translation (50). The effect of the poly(A) tail on translation is facilitated by PABP (56). The interaction between

PABP and eIF4G brings about the circularization of the mRNA that explains the synergism between cap and poly(A) in enhancing initiation of translation (50). It has been proposed that (62) such circularization of the mRNA enhances translation either via stimulating the interaction of eI4E with the cap or via shunting terminating ribosomes to the 5' end of the mRNA. In yeast systems, RNA transfection experiments showed that polyadenylated RNA is translated at a much higher rate than RNA missing a poly (A) tail (63). This confirms that there is an interaction between the 5’ and 3’ end of the mRNA and poly (A) tail and cap structure act synergistically. Hence, the rate of translation of an RNA possessing both a cap and a poly(A) tail is much higher than the sum of translation rates of RNA carrying either modification by itself (51). Poly(A) tails have also been observed in prokaryotes. In prokaryotic systems, however, the role of poly (A) tail is quite different. Poly (A) tail triggers degradation of mRNA in prokaryotes (57).

1.8 Fluorescence anisotropy

Fluorescence anisotropy, especially over the past 10 years, is a widely used technique in biophysical research. It is being used to study protein ligand association reactions, protein denaturation, and the rotational rates of proteins.

If you irradiate a perfectly oriented, immobilized fluorescent sample with polarized light parallel to the absorption transition dipole, their emission is polarized. The extent to which the fluorescence anisotropy is decreased or increased is strongly dependent on the rate at which the molecule rotates or tumbles.

The strategy for measuring fluorescence anisotropy is suggested by the Figure.3 below. A sample is excited with linearly polarized light. Fluorescence intensity measurements are made with an emission polarizer oriented either perpendicular or parallel to the plane of polarization of the incident beam. Anisotropy (symbolized either *A* or *r*) is defined as

$$r = A = \frac{I_{\parallel} - I_{\perp}}{I_{\parallel} + 2I_{\perp}}$$

where the I terms denote intensity measurements parallel ($I_{\parallel}$) and perpendicular ($I_{\perp}$) to the incident polarization.

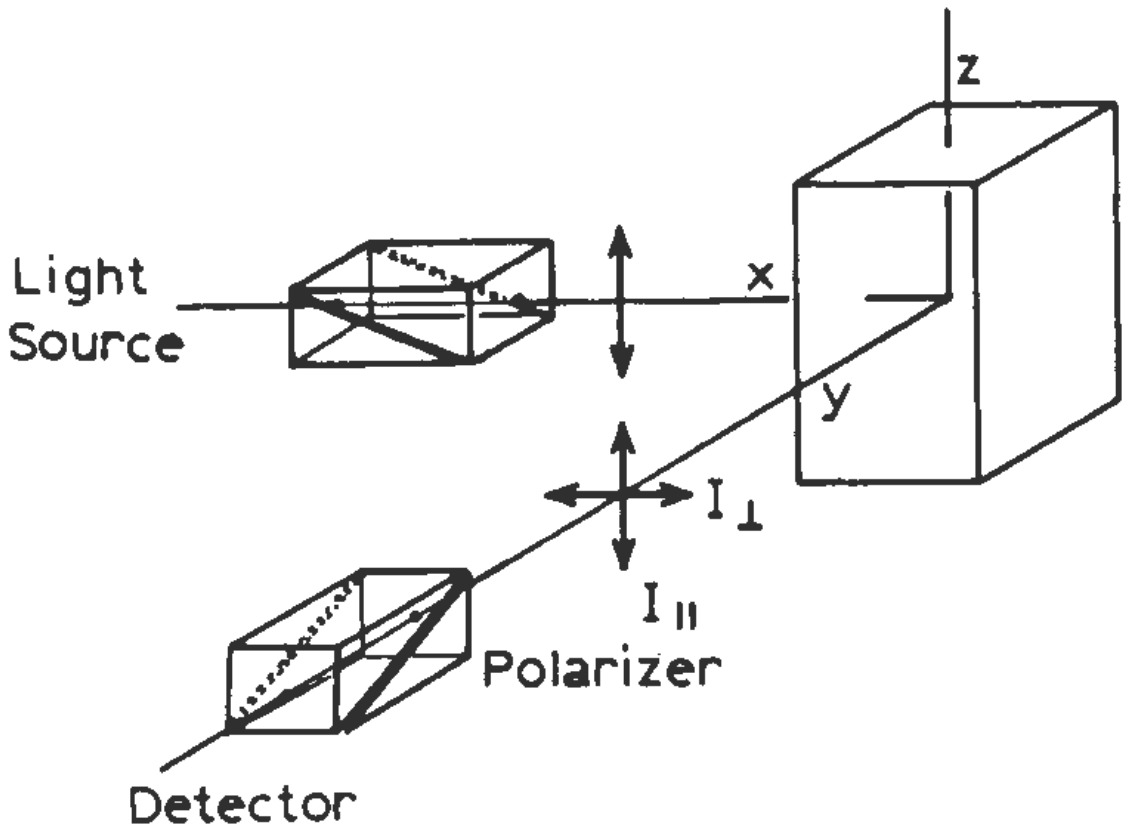

Figure 3. Fluorescence anisotropy measurement

2.0 Material and Methods

2.1 Materials

5' fluorescein (FL) labeled pseudoknot PK1 RNA (^{Fl}PK1) and Poly $(A)_{20}$ were synthesized by Gene Link, Inc. Hawthorne, New York. PK1 domain(FLCAAAACAAACGAAUCUCAAGCAAUCAAGCAUUCUACUUC UAUUGCAGCAA) was used for RNA binding studies as described previously (19).

2.2 Purification of eIF4F from Wheat Germ

Wheat germ eIF4F was isolated from the 0-40% ammonium sulfate fraction of the 120 mM KCl post-ribosomal supernatant fraction as described elsewhere (3). Briefly, 300 ml DEAE-cellulose column equilibrated in buffer B-40 was loaded with the 0-40% ammonium sulfate fraction. The column was washed with buffer B-40 until the optical density returned to the baseline. 40 to 150 mM linear KCl gradient develop in buffer B containing 20 mM HEPES/KOH, pH 7.6, 1 mM DTT, 0.1 mM EDTA, and 5% glycerol. The column was washed with buffer B-150 followed by developing with a second 150 to 300 mM linear KCl gradient in buffer B. 10 ml Fractions were collected in sterilized falcon tubes. The aliquots containing eIF4F fractions were pooled. After dialyzing with buffer B-40, fractions were loaded to a HiTrap SP column. The dialyzed sample was loaded to a 5 ml HiTrap SP column equilibrated in buffer B-40. After

applying samples, the column was washed with buffer B-40 and then developed with a 40 to 400 mM linear KCl gradient in buffer B. 1 ml Fractions were collected in eppendorf tubes. eIF4F elutes in 250 mM KCl. The active fractions confirmed by binding assays were pooled and dialyzed in buffer B-40. After overnight dialyzing, the samples were applied to 2 ml m^7GTP-sepharose column equilibrated in buffer B-40. The column was washed with buffer 50 ml B-40, followed by buffer B-40 containing 0.1 mM GTP. Retained eIF4F was eluted with B-40 containing 100 mM GTP. The active fractions were pooled and concentrated in a Centricon-10 microconcentrator (Amicon Corp.). Purity of protein was confirmed by running 7.5% SDS-polyacrylamide gel electrophoresis. The concentration was determined by a Bradford assay using bovine serum albumin (BSA) as standard.

2.3 Expression and Purification of eIF4B

eIF4B was expressed in *Escherichia coli* containing the constructed pET3d vector in BL21(DE3) pLys as described elsewhere (1) A HiTrap SP column (Amersham Pharmacia Biotech) was used to purify eIF4B by the following procedure. E. coli cells were disrupted by sonicator. Disrupted cells were suspended in buffer B-600 [20 mM Hepes/KOH (pH 7.5), 1 mM DTT, 0.1 mM EDTA, 10% glycerol, and 600 mM KCl] containing 0.5 mM phenylmethanesulfonyl fluoride (PMSF), 0.5 mL of aprotinin, and 100 μg/mL soybean trypsin inhibitor. After centrifugation of disrupted cells at 45 000 rpm

for 2h, the supernatant was dialyzed against buffer B-50 and loaded onto a 5 mL HiTrap SP column. The column was washed with B-50 buffer until the absorbance reached the baseline. To elute eIF4B protein, 50 to 400 mM KCl linear gradient (total volume of 100 mL) was used. 1.0 mL protein fractions were collected in eppendorf tubes. The protein band started to appear in the 200-300 mM KCl fractions. The purity of the protein was confirmed by 10% SDS-PAGE gel. All purification steps were performed in a cold box at approximately 4 °C.

2.4 Expression and Purification of PABP

PABP was expressed in *Escherichia coli* containing the constructed pET19b vector in BL21 (DE3) pLysS. Cells were expressed in Luria Bertani (LB) medium containing 34 µg/ml chloramphenicol and 100 µg/ml ampicillin at 37 °C. When the optical density reached 0.5 at 600 nm, expressed cells were induced for 5 h with 0.1g/L isopropyl-1-thio-β-D-galactopyranoside (IPTG). After this step, all experiments were carried out at 4 °C .The cells were harvested by centrifugation and pellets were resuspended into binding buffer (20 mM Tris-HCl, (pH 7.9) 0.5 M NaCl, and 5 mM imidazole) including 100 µg/ml soybean trypsin inhibitor, 0.5 ml of aprotinin and 1.0 mM phenylmethylsulfonyl fluoride (PMSF). Subsequently, cells were disrupted by sonication for 30 seconds intervals for 5 times and the lysate was centrifuged. Supernatant was passed through a 5 ml His-bind nickel column previously equilibrated with binding buffer. The column was washed with binding buffer.

Using elution buffer, 20 mM Tris-HCl, pH 7.9, 0.5 M NaCl, and 200 mM imidazole, the bound protein was eluted. The eluted protein was dialyzed against buffer (20 mM Tris-HCl, pH 7.6, 150 mM NaCl, and 5% glycerol). The purity of the PABP was confirmed by 10% SDS-PAGE.

All protein samples were dialyzed against Titration Buffer (20 mM Tris-HCl, pH 7.6, 150 mM KCl, 2.0 mM $MgCl_2$, and 1.0 mM DTT) and passed through a 0.22 μM filter (Millipore) prior to the spectroscopy measurement. The proteins were concentrated with a Centricon 10 (Amicon Co.) filter. The protein concentrations were determined by a Bradford assay with bovine serum albumin as the standard [41] using a Bio-Rad protein assay reagent (Bio-Rad Laboratories, Hercules, CA).

2.5 Fluorescence Anisotropy Measurements

Fluorescence anisotropy measurements were carried out using a Spex Fluorolog τ2 spectrofluorimeter equipped with excitation and emission polarizers. Anisotropy experiments were performed using an L-format detection configuration. Direct fluorescence anisotropy titration was employed to study protein-RNA (eIFs-PK1) interactions. The 50 nM 5' fluorescein labeled PK1 RNA (^{FI}PK1) was incubated with varying concentrations of eIF4F, eIF4F·Poly(A)$_{20}$, eIF4B, eIF4B·Poly(A)$_{20,}$ PABP, PABP ·Poly(A)$_{20,}$ eIF4F·4B, eIF4F·4B·Poly(A)$_{20,}$ eIF4F·PABP, eIF4F·PABP·Poly(A)$_{20,}$ eIF4F·4B·PABP, and eIF4F·4B·PABP·Poly(A)$_{20}$ complex (0-1.1 μM) in titration buffer. Prior to anisotropy measurements, all samples were incubated

at least 15 min. The sample temperature was maintained at 25 °C for all experiments unless otherwise noted.

In order to study the temperature dependence of the protein-RNA interaction, the samples were thermostated at different temperatures as described in Results. The temperature was measured using a thermocouple inside the cuvette. Interaction of initiation factors (eIFs) with ^{FI}PK1 was measured by the enhancement in anisotropy of ^{FI}PK1 RNA emission. The anisotropy values of each sample were recorded by excitation with vertically polarized light at wavelength of 490 nm and the emission was measured at 519 nm in the horizontal and vertical directions. The anisotropy data was fitted to equation 1 to determine the dissociation equilibrium constant (42, 43).

$$r_{obs} = r_{min} + \{(r_{max} - r_{min})/(2 \times [^{FI}PK1])\}\{b - (b^2 - 4\,[^{FI}PK1]\,[eIFs])\text{^}\,0.5\} \qquad \text{(Eq 1)}$$

where, $b = K_d + [^{FI}PK1] + [eIFs]$, r_{obs} is the observed anisotropy for any point in the titration curve, r_{min} is the minimum observed anisotropy in the absence of protein, r_{max} is the maximum anisotropy at saturation, $[^{FI}PK1]$ and [eIFs] are the PK1 RNA and protein concentrations. K_d is the equilibrium dissociation constant. Employing KaleidaGraph software (version 4.01), nonlinear least squares fitting of the titration data was carried out.

2.6 Protein Complexes

To measure protein-protein interactions, complex formation was examined by monitoring changes in intrinsic protein fluorescence. The titration data showed that K_d values of eIF4F·PABP, eIF4F·eIF4B, and eIF4F·4B·PABP were 43 nM, 62 nM and 32 nM, respectively. K_d values of eIF4F·Poly$(A)_{20}$, eIF4B·Poly$(A)_{20}$, and PABP·Poly$(A)_{20}$ were 317 nM, 59 nM, and 16 nM, respectively. K_d values of eIF4F·PABP·Poly$(A)_{20,}$ eIF4F·4B·Poly$(A)_{20}$, and eIF4F·4B·PABP·Poly$(A)_{20}$ were 23 nM, 51 nM, and 13 nM, respectively.

Using these K_d values, calculations were performed so that more than 90% of the eIF4F and Poly$(A)_{20}$ were in the complex at the lowest protein titration point, 50 nM. The molar ratio of eIF4F (1 μM) to PABP (10 μM) or eIF4B (10 μM) in the binding reaction was 1:10, while the ratio of eIF4F·4B·PABP was 1:10:30. For Poly$(A)_{20}$ experiments, the molar ratio of eIF4F·Poly$(A)_{20}$, eIF4B·Poly$(A)_{20}$, and PABP·Poly$(A)_{20}$ were 1:25, 1:10, and 1:5, respectively. The molar ratio of eIF4F·4B, eIF4F·PABP, eIF4F·4B·PABP to Poly$(A)_{20}$ were 1:10, 1:5, and 1:6, respectively. To ensure protein complex formation, the samples were incubated for 15 minutes.

2.7 Thermodynamic Parameters for Initiation Factors in the presence and absence of Poly$(A)_{20}$ with PK1 RNA

Temperature dependent thermodynamic parameters, enthalpy change (ΔH), entropy change (ΔS), and free energy change (ΔG), were determined using the following equations:

$$-RT\ln K_{eq} = \Delta H - T\Delta S \qquad \text{(Eq 2)}$$

$$\Delta G = -RT\ln K_{eq} \qquad \text{(Eq 3)}$$

In the equations above, R and T are the universal gas constant and absolute temperature, respectively. K_{eq} is the dissociation equilibrium constant and was obtained at different temperatures. ΔH and ΔS were obtained from the slope and intercept, respectively, of the plot $-\ln K_{eq}$ versus 1/T while ΔG was determined from equation (3)

2.8 Stopped-Flow Fluorescence Anisotropy Measurements

Stopped-Flow fluorescence anisotropy experiments were performed on an OLIS RSM 1000 stopped-flow spectrophotometer equipped with a fluorescence of polarization module with a dead time. The dead time, the age of the mixture when it is first available for measurement, is 1ms. The excitation wavelength for fluorescein level pseudoknot RNA (^{FI}PK1 RNA) was 490 nm.

The time dependent change in fluorescein emission was monitored at 520 nm by using a cut-off filter. By using a temperature-controlled circulating water bath, the temperature of the flow cell and solution reservoirs was sustained at 25 °C. After the rapid mixing of samples, the time course of fluorescence anisotropy change was measured by computer data acquisition. In each experiment, 1000 data points were collected per rapid-mix shot, and sets of data from 5-10 experiments were averaged. Each averaged set of stopped-flow data was then fitted by nonlinear least squares fitting using Kaleidagraph (4.01, Synergy Software, West Palm Beach, FL) to the following single (Eq 4) and double (Eq 5) exponential equations.

$$r_t = \Delta r \exp(- k_{obs} . t) + r_{final} \qquad \text{(Eq 4)}$$

$$r_t = \Delta r_1 \exp(-k_{obs1} . t) + \Delta r_2 \exp(-k_{obs2} . t) + r_{final} \qquad \text{(Eq 5)}$$

where r_t is the observed anisotropy at any time, t, Δr is the amplitude and k_{obs} is the observed first order rate constant, r_{final} is the anisotropy at the equilibrium in the reaction, and Δr_1 and Δr_2 are the amplitudes for observed rate constants k_{obs1} and k_{obs2}, respectively.

3.0 Results

The first quantitative data (24) on the binding interactions of plant protein synthesis initiation factors with IRES was determined in our lab and it has been showed that the TEV leader can discriminate between eIF4G isoforms to preferentially recruit one isoform over the other. Zeenko and Gallie (19) demonstrated that the PK1 within the TEV leader was necessary for cap-independent translation and eIF4G subunit of eIF4F was required. Further, the binding efficiency of PK1 with 20 nM eIF4G and 200 nM eIFiso4G was studied. These concentrations were chosen from preliminary studies so that the concentration of protein was less than K_d. The binding plots are shown in Figure 4 (24). The dissociation constants, $K_{d,}$ for eIF4G and eIFiso4G binding to PK1 RNA were 0.126 ± 0.01 and 3.85 ± 0.7 μM, respectively. This result showed that eIF4G bound PK1 with 30-fold higher affinity than eIFiso4G (Table 1). Binding affinity of eIF4F and eIFiso4F to PK1 RNA was also studied. 20 nM wheat germ eIF4F or 200 nM eIFiso4F were titrated with PK1 RNA. The binding plots are shown in Figure 5 (24). eIF4F bound PK1 with ~3.5-fold greater affinity than eIFiso4F. The presence of eIF4E, the cap-binding protein, had very small effect on eIF4G binding affinity. On the other hand, eIFiso4E enhanced the affinity of eIFiso4G when present as part of the eIFiso4F complex. The results showed that eIFiso4F bound to PK1 RNA ~6-fold more strongly than did eIFiso4G while the binding of eIF4F and eIF4G were very similar

(Table 1). The presence of the cap-binding proteins, eIFiso4E and eIF4E, decreased the discrimination between the two eIF4F isoforms by almost 9-fold.

In order to determine whether or not there were notable differences between binding to PK1 versus the full-length TEV leader, the binding affinity to TEV1–143 with eIFiso4F (Figure 6) and eIF4F (Figure 7) were studied. The binding affinity of eIFiso4F and eIF4F to TEV1–143 full length demonstrated the same pattern as observed for PK1 with K_d of 0.178 ± 0.03 and 0.079 ± 0.01 μM, respectively. eIF4F binding to the TEV1–143 was 2.3 times tighter than eIFiso4F while the difference in binding affinity between the two proteins was 3.5-fold for PK1. K_d for eIFiso4G and eIF4G binding to the full-length TEV leader was 2.25 ± 0.33 and 0.10 ± 0.01 μM, respectively. This showed that eIF4G bound TEV1–143 with greater than 20-fold higher affinity than did eIFiso4G. These results resemble binding of proteins to PK1 alone where the difference was ~30-fold. While the binding of eIF4G to TEV1–143 and PK1 was the same within experimental error, binding of eIFiso4G to TEV1–143 increased slightly.

It has been shown (19) that mutation of loop 3 within PK1, so called S1–3, reduced cap-independent translation to ~7.4% of wild-type levels. To understand whether the mutation in S1–3 that significantly decreases cap-independent translation also reduces eIF4F and eIFiso4F binding, the binding of eIFiso4F and eIF4F to S1–3 RNA (Figure 7, 8) was studied. The binding of eIFiso4F (and IFiso4G) to S1–3 was reduced as least 10-fold when compared

with binding to TEV1–143 (Table 1). eIF4F (and eIF4G) showed 6-fold less binding affinity to S1–3 compared with binding to TEV1–143. Since binding of eIF4F showed similar pattern for binding to PK1 and TEV1–143, PK1 was used for our further analyses.

Table. 1: Dissociation Constant, (K_d) for the interaction of eukaryotic initiation factor proteins with TEV 1-143, pseudo knot PK1 and mutant S1-3 of PK1 mRNA of TEV 5'-leader at 25°C.

Proteins	**TEV 1-143** (K_d in μM)	**PK1** (K_d in μM)	**S1-3** (K_d in μM)
eIF(iso)4G	2.25 ±0.33	3.85 ±0.7	>20
eIF4G	0.10 ±0.01	0.126 ±0.01	0.586 ±0.04
eIF(iso)4F	0.178 ±0.03	0.685± 0.06	2.03 ± 0.21
eIF4F	0.079 ±0.01	0.194 ±0.01	0.502 ±0.05

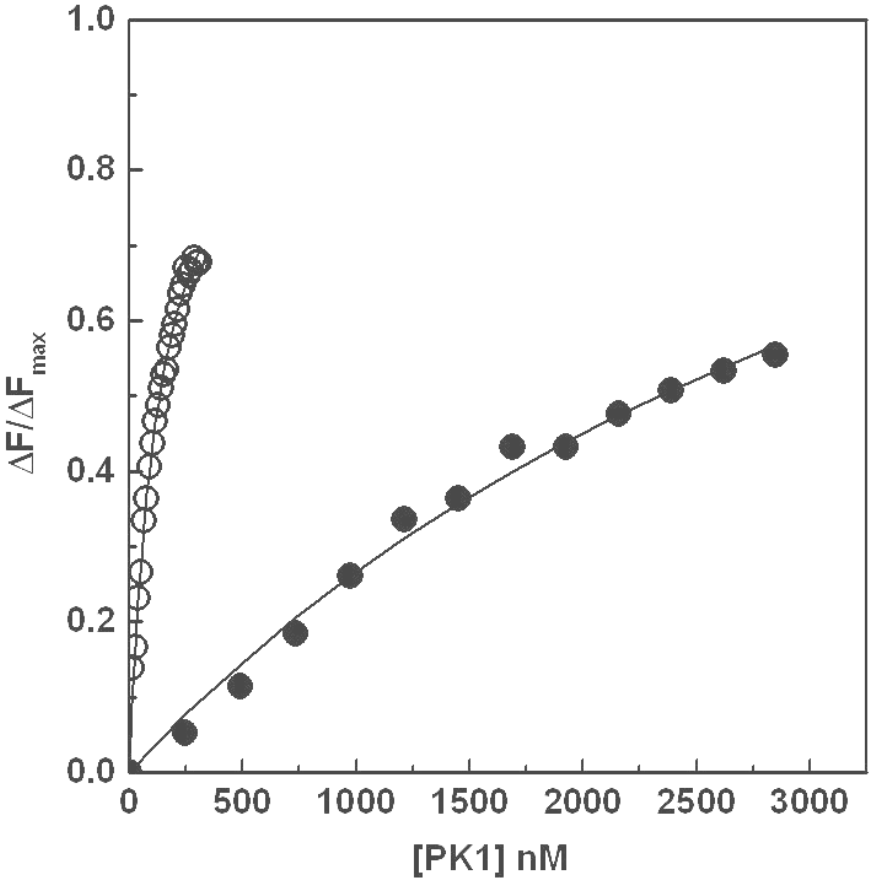

Figure 4. Binding plots of eIF4G (20 nM) and eIFiso4G (0.2 μM) with PK1 RNA in titration buffer (10 mM Tris-HCl, 150 mM KCl pH 7.5) at 25 °C. Fluorescence emission intensity was measured at 333 nm and excitation was at 280 nm. ΔF_{max} is the fluorescence change for complete saturation of protein with ligand. The values of $\Delta F/\Delta F_{max}$ for eIFiso4G (•) and eIF4G (○) versus concentration of PK1 are shown (24).

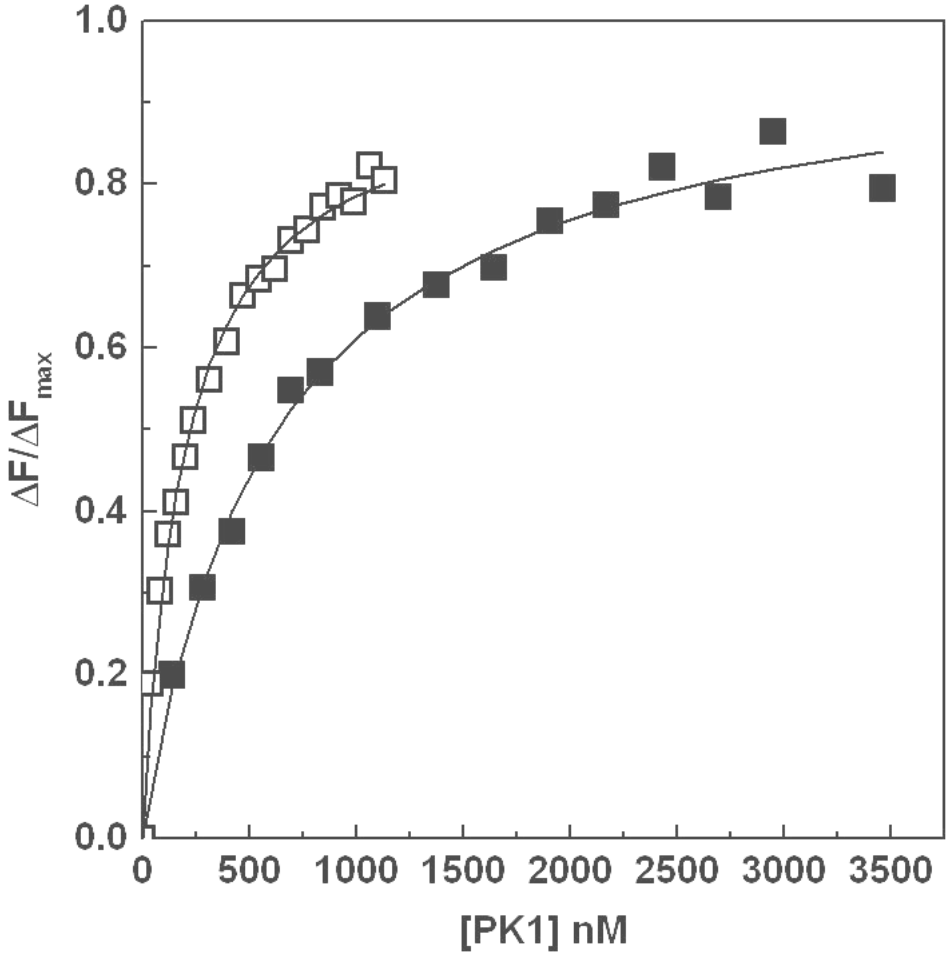

Figure 5. Binding plots of eIF4F (20 nM) and (0.2 μM) eIFiso4F with PK1 RNA) at 25 °C. The values of $\Delta F/\Delta F_{max}$ for eIFiso4F (■) and eIF4F (□) versus concentration of PK1 RNA are shown. eIFiso4F was prepared by incubation of recombinant 0.1 μM eIFiso4G (86 kDa) and 0.1 μM eIFiso4E (28 kDa) for 15 min at 4 °C (24). Experimental conditions were as described for Fig 4.

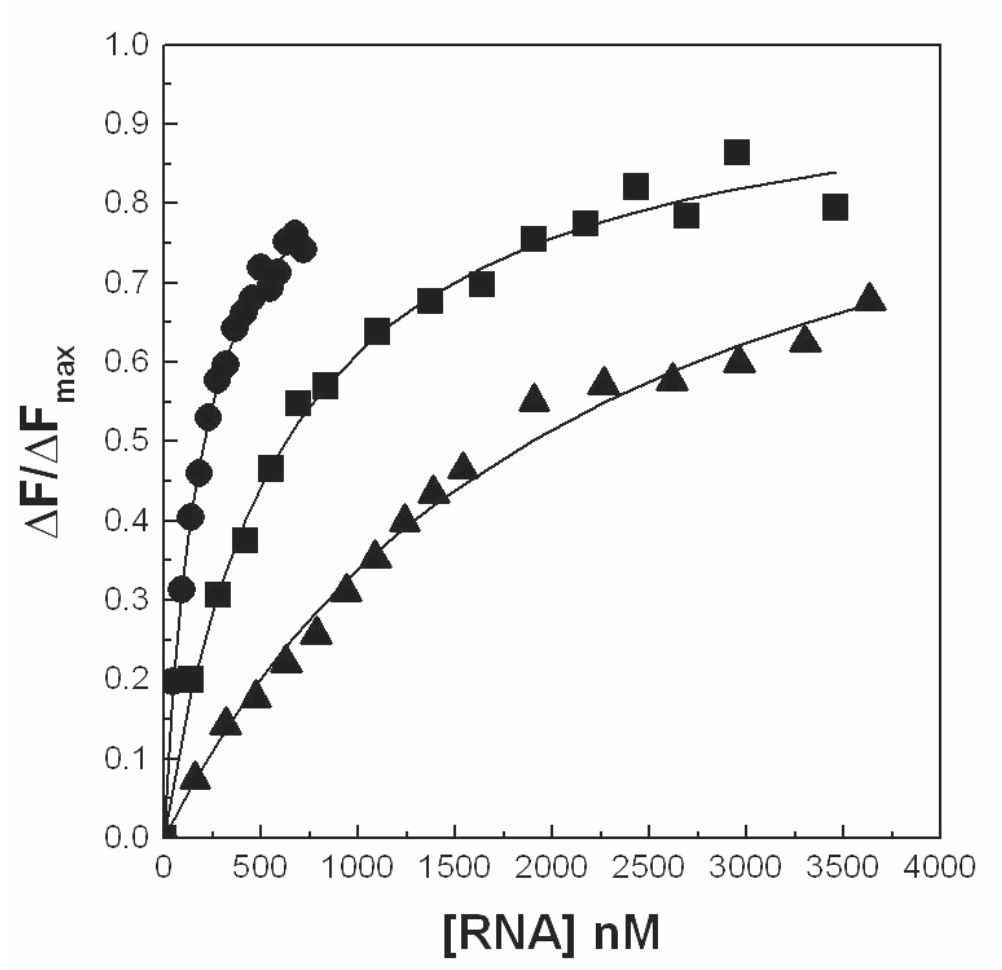

Figure 6. Binding analysis of eIFiso4F with TEV1–143, PK1, and S1–3 RNA) at 25 °C. $\Delta F/\Delta F_{max}$ plots for eIFiso4F (0.2 μM) against the concentrations of TEV1–143 (•), PK1 (■), and S1–3 (▲) are shown (24). Experimental conditions were as described for Fig 4.

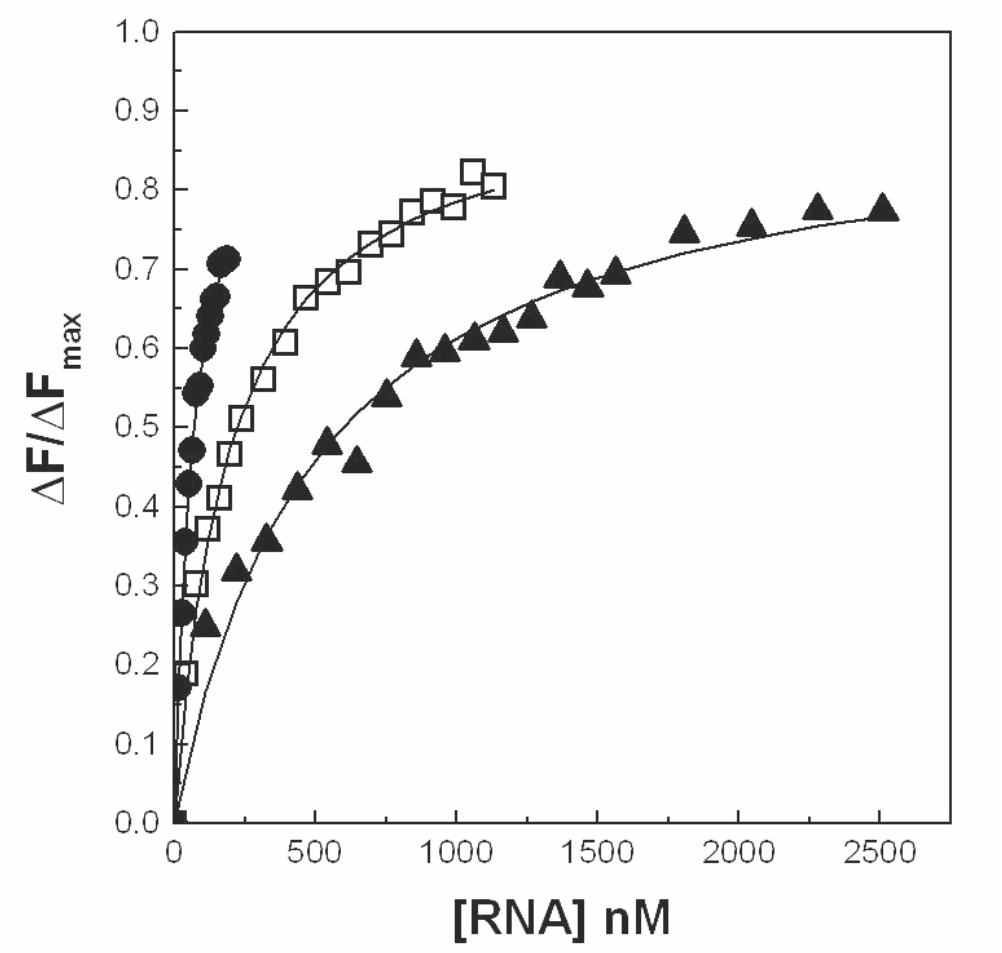

Figure 7. Binding analysis of eIF4F with TEV1–143, PK1, and S1–3 RNA) at 25 °C. $\Delta F/\Delta F_{max}$ plots for eIF4F (20 nM) against the concentrations of TEV1–143 (•), PK1 (□), and mutant S1–3 (▲) are shown (24). Experimental conditions were as described for Fig 4.

3.1 eIF4F Binding to Fluorescein Labeled PK1 RNA

Because of the high absorbance of the RNA, corrections for the inner filter effect were necessary. In order to eliminate inner filter corrections, 5' fluorescein labeled PK1 RNA, ^{FI}PK1, has been used in our further studies. To see if labeling PK1 RNA with a fluorescein tag causes a dramatic change to binding of eIF4F, we studied fluorescent anisotropy measurements for eIF4F binding to ^{FI}PK1 RNA. The binding of 50 nM ^{FI}PK1 RNA with eIF4F (Figure 8) at 25 ° is shown. The observed anisotropy change, r_{obs}, of PK1 RNA was plotted versus the concentration of protein. The line indicates the fitted curves. The data were fitted to equation 1. K_d value was acquired using a non-linear least squares analysis described elsewhere (58, 59). K_d of eIF4F-PK1 RNA was found to be 203 ± 14 nM. Scatchard analysis demonstrated that eIF4F bound to a single PK1 RNA (data not shown). These data showed that fluorescein labeled PK1 RNA (203 ± 14 nM) and unlabeled PK1 RNA (194 ± 10 nM) had the same affinity for eIF4F. For further analysis, 5' fluorescein labeled PK1 RNA was used. Binding of eIF4F to the PK1 RNA at different temperatures ,15 °C, 10 °C, and 5 °C, was also studied (Table 2).

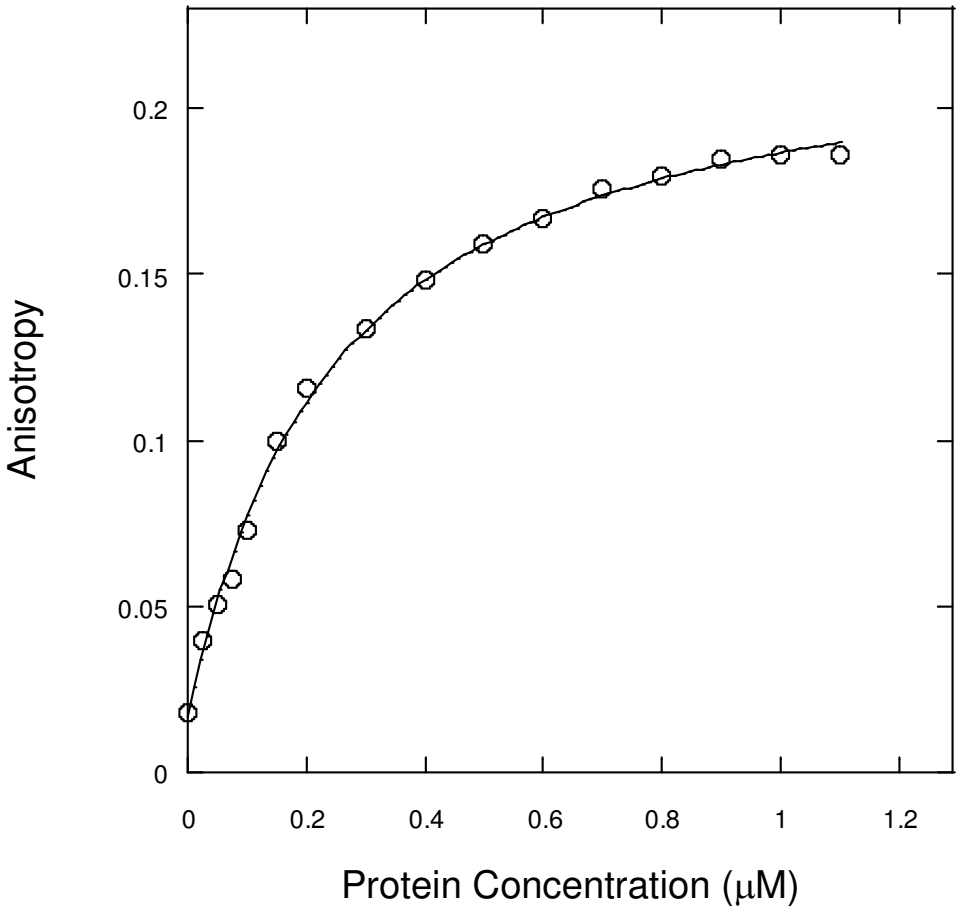

Figure 8. Fluorescence anisotropy measurements for addition of eIF4F to fluorescein labeled PK1(^{Fl}PK1) RNA at 25 °C . The excitation and emission wavelengths were 490 and 519 nm, respectively. PK1 concentration was 50 nM in Titration buffer (20 mM Tris-HCl, pH 7.6,150 mM KCl, 2.0 mM $MgCl_2$, and 1.0 mM DTT).

3.2 Effect of eIF4B on eIF4F Binding to PK1 RNA

eIF4B has multiple roles through interactions with several initiation factors and RNA to facilitate translation initiation. It stabilizes eIF4F binding to the 5' cap, PABP binding to the poly(A) tail, and mRNA binding to ribosomes. Since eIF4B stabilizes eIF4F binding to cap, it has been determined whether eIF4B had an effect on binding of eIF4F to fluorescein labeled PK1 RNA, which lacks a cap structure. The fluorescence anisotropy measurements for binding of PK1 RNA with eIF4F in the presence and absence of eIF4B were studied and 50nM PK1 RNA was titrated with eIF4F, eIF4F·4B and eIF4B. The binding of fluorescein labeled PK1 RNA with eIF4F, eIF4F·4B, and eIF4B at 25 °C is shown in Figure 9. The observed anisotropy change r_{obs} of PK1 RNA was plotted versus the concentration of proteins. The lines indicate the fitted curves. The data were fitted to equation 1, and the dissociation constant, K_d , values were determined. K_d for eIF4F and eIF4F-4B binding to PK1 RNA was 203 ± 14 and 95 ± 5 nM, respectively. This result showed that eIF4B enhanced the affinity of eIF4F to PK1; eIF4F-4B bound to PK1 2 fold more strongly than did eIF4F. Binding of eIF4B alone to PK1 RNA was also studied. K_d for eIF4B (1383 ± 93 nM) binding to PK1 was about 6.8 fold lower affinity (higher K_d) than eIF4F binding to PK1 RNA. Binding of eIF4F·4B to the PK1 RNA at different temperatures 15 °C, 10 °C, and 5 °C, was also studied (Table 2).

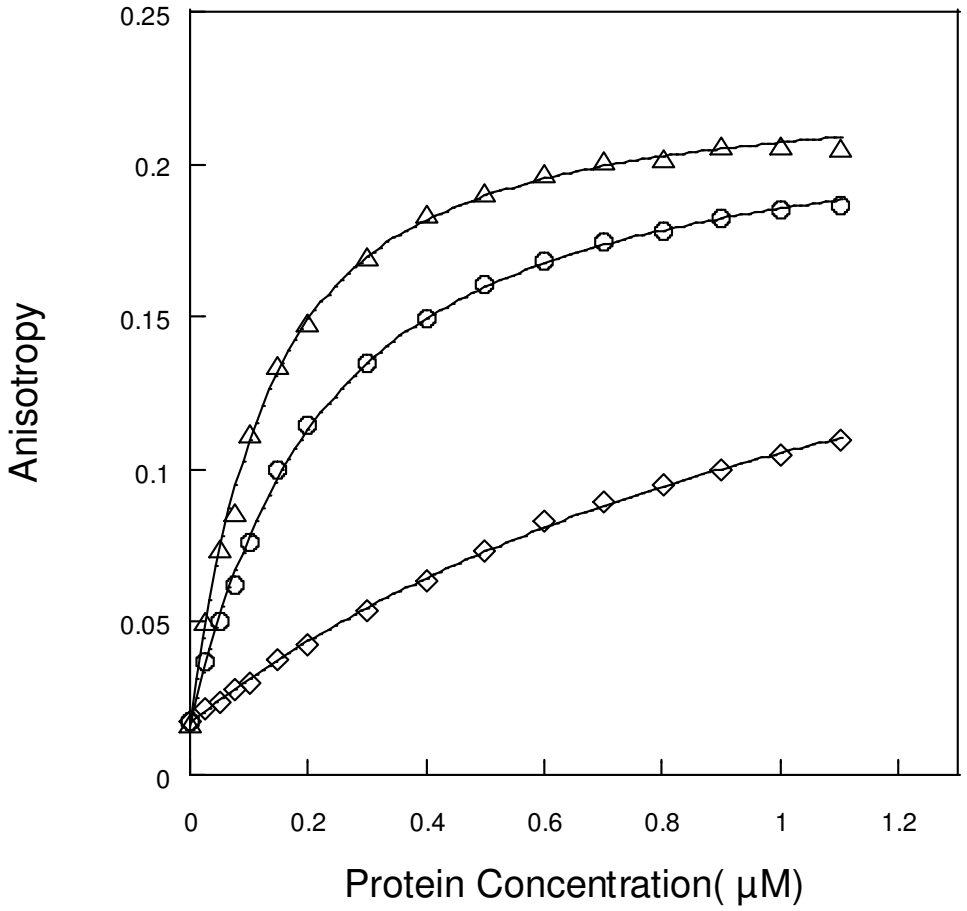

Figure 9. Fluorescence anisotropy measurements for the binding of 50 nM ^{FI}PK1 RNA with eIF4F, eIF4F·4B, and eIF4B. The anisotropy values of eIF4F-PK1 (—O—), eIF4F·4B-PK1 (—Δ—) and eIF4B-PK1 (—□—) are shown. Experimental conditions were as described for Fig.9. eIF4F·4B (1:10) complex was prepared by incubation of 1 µM eIF4 and 10 µM eIF4B for 15 min at 4 °C. 88% of the eIF4F was associated in the complex.

3.3 Effect of PABP on eIF4F and eIF4F·4B Binding to PK1 RNA

After studying the effect of eIF4B on binding activity of eIF4F to PK1 and determining the dissociation constants, the fluorescence anisotropy measurements for binding of fluorescein labeled PK1 RNA with eIF4F in the presence and absence of PABP were studied. 50nm fluorescein labeled PK1 RNA titrated with PABP and eIF4F·PABP. Figure 10 shows the binding of PK1 RNA with eIF4F, eIF4F·PABP, and PABP at 25 °C. The observed anisotropy change r_{obs} of PK1 RNA was plotted versus the concentration of proteins. The lines indicate the fitted curves. The data were fitted to equation 1, and the dissociation constant, $K_{d,}$ values were determined. K_d for eIF4F·PABP and PABP binding to PK1 RNA was 113 ± 9 nM and 1765 ± 99 nM, respectively. This result demonstrates that PABP enhanced the affinity of eIF4F to PK1 almost 2 fold which indicates an effect similar to that of eIF4B. The results of binding of eIF4F· PABP to the PK1 RNA at different temperatures 15 °C, 10 °C, and 5 °C, are shown in Table 2.

Further, the binding affinity of eIF4F with PK1 RNA was analyzed when both PABP and eIF4B were present. The results of the titration data revealed that binding affinity of eIF4F was enhanced about 4-fold toward PK1 RNA in the presence of both PABP and eIF4B. K_d of eIF4F·4B·PABP binding to PK1 RNA was 51 ± 2.5 nM (Table 2).

Figure 11 shows the binding analyses of PK1 RNA with eIF4F·4B, eIF4F·4B· PABP, and eIF4B at 25 °C.

Effect of the temperature on eIF4F·4B· PABP binding to PK1 RNA has also been studied. The data for binding assays of eIF4F·4B· PABP with PK1 RNA at different temperatures, 15 °C, 10 °C, and 5 °C are shown in Table 2.

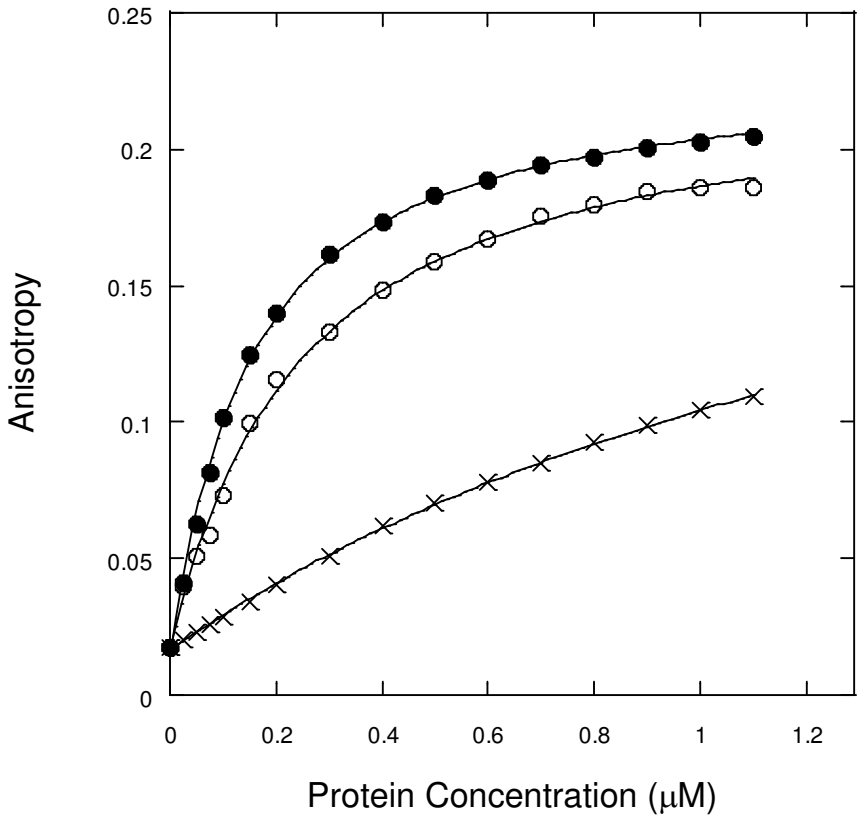

Figure 10. Fluorescence anisotropy for the binding of ^{FI}PK1 RNA with eIF4F and eIF4F·PABP and PABP at 25 °C. The anisotropy values of eIF4F-PK1 (—O—), eIF4F·PABP-PK1(—•—)and PABP-PK1 (— X—) are shown. The ^{FI}PK1 RNA concentration was 50 nM in Titration Buffer. Experimental conditions were as described for Fig. 9. 10 μM PABP was incubated with 1 μM eIF4F for 15 min to prepare eIF4F·PABP complex. 91% of the eIF4F was associated in the complex.

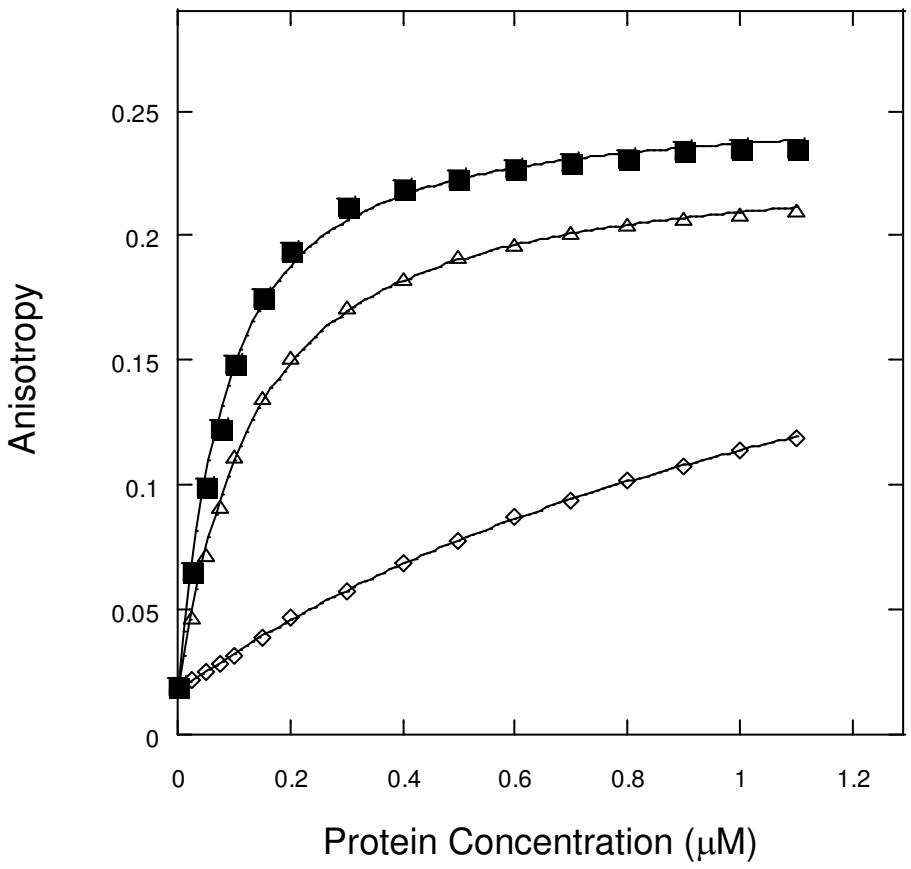

Figure 11. Fluorescence anisotropy measurements for the binding of ^{FI}PK1 RNA with eIF4B, eIF4F·4B and eIF4F·4B·PABP. The anisotropy values of eIF4B-PK1 (—□ —), eIF4F·4B-PK1 (—Δ—), and eIF4F·4B·PABP-PK1 (—■—) are shown at 25 °C. Experimental conditions were as described for Fig. 9. 1 μM eIF4F, 10 μM eIF4B and 30 μM PABP were incubated for 15 min at 4 °C to prepare eIF4F·4B and eIF4F·4B·PABP complexes. 88% (eIF4F·4B) and 96% (eIF4F·4B·PABP) of the eIF4F was associated in the complex.

Table 2. Equilibrium dissociation constants (K_d) for the interaction of eIF4F, eIF4F·PABP, eIF4F·4B, and eIF4F·4B·PABP with fluorescein tag PK1 RNA (^{FI}PK1).

Complex	PK1 25 ºC (K_d nM)	PK1 15 ºC (K_d nM)	PK1 10 ºC (K_d nM)	PK1 5 ºC (K_d nM)
eIF4F-PK1	203 ±14	170 ± 13	151 ± 1	128 ± 12
eIF4F·4B-PK1	95 ± 5	72 ± 6	63 ± 4	52 ± 3
eIF4F·PABP-PK1	113 ± 9	86.6 ± 4.3	66.9 ± 3.3	60.5 ± 3.6
eIF4F·4B·PABP-PK1	51 ± 2.5	38.2 ± 2.4	31.6 ± 1.9	22.7 ± 2.2
eIF4B-PK1	1383 ± 93			
PABP-PK1	1765 ± 99			

3.4 Temperature Effect on the binding of eIF4F, eIF4F·4B, and eIF4F·4B·PABP with PK1 RNA

A Van't Hoff plot of ln K_{eq} versus the reciprocal of temperature (1/T) was used to calculate the thermodynamic parameters of enthalpy (ΔH) and entropy (ΔS) (Fig. 12). The values of ΔH and ΔS were obtained from the slope and intercept, respectively and are shown in Table 3. The ΔG values at 25 °C were calculated from equation 3 and are shown in Table 3. The results showed that eIF4F-PK1, eIF4F·4B-PK1, eIF4F·PABP-PK1 interactions are both enthalpically and entropically favorable. This suggests hydrophobic interactions may play a role in binding. This may happen through interactions either with the RNA or through conformational changes in the protein. While addition of eIF4B seems to have little effect on the entropic contribution, addition of PABP decreases the entropic contribution. PABP causes the enhancement of enthalpic contribution. In the case of addition of eIF4B·PABP complex to eIF4F, it was observed that addition of the complex significantly lowers the entropic contribution (ΔS = 26.6 ± 1.8) for PK1 binding. The relatively small entropic contributions to the protein complex of eIF4F·eIF4B·PABP to PK1 RNA suggest that hydrophobic residues are more solvent exposed in the combined structure. In conclusion, formation of protein complex favors hydrophobic interactions and RNA binding is primarily enthalpic.

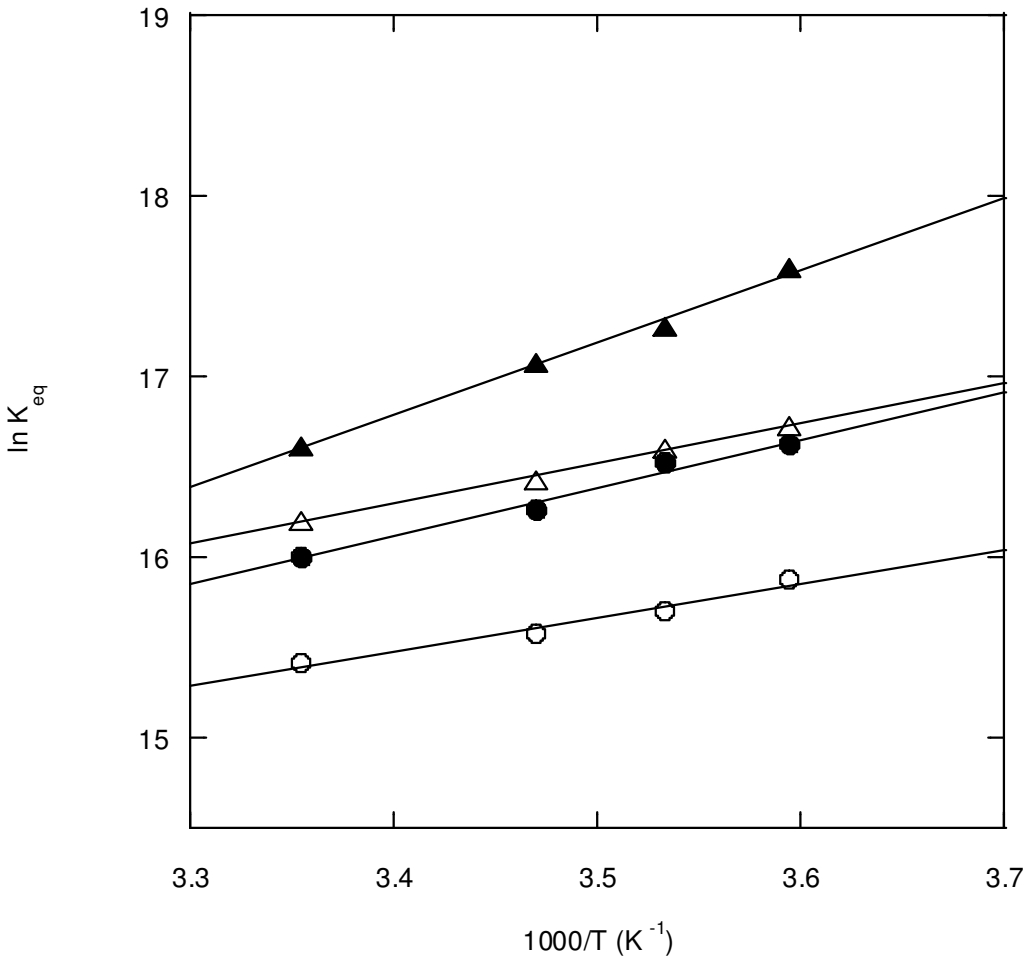

Figure 12.Van't Hoff plots for the interaction of ^{FI}PK1 RNA with translation initiation factors. The data are indicated as eIF4F-PK1 (—O—), eIF4F·PABP-PK1 (—●—), eIF4F·4B-PK1 (—Δ—) and eIF4F·4B·PABP-PK1 (—▲—).Enthalpy (ΔH) and entropy (ΔS) were calculated from the slope and intercept of the temperature dependent equilibrium binding measurements, respectively.

Table3.Thermodynamic parameters of enthalpy, entropy and free energy change for the interactions of eukaryotic initiation factors complex with ^{FI}PK1 RNA.

Complex	ΔH (kJ mol^{-1})	ΔS (J $mol^{-1}K^{-1}$)	ΔG (kJ mol^{-1})
eIF4F-PK1	-15.5 ± 1.5	76.0 ± 3.6	-38.18 ± 0.17
eIF4F·4B-PK1	-18.5 ± 1.3	72.6 ± 6.4	-40.06 ± 0.13
eIF4F·PABP-PK1	-22.3 ± 1.2	58.3 ± 3.7	-39.62 ± 0.18
eIF4F·4B·PABP-PK1	-33.2 ± 2.2	26.6 ± 1.8	-41.60 ± 0.11

3.5 Effect of Poly$(A)_{20}$ on eIF4F, eIF4F·4B, and eIF4F·eIF4B·PABP Binding to PK1 RNA

After determining the effect of PABP on eIF4F, eIF4F·4B binding to PK1 RNA, it has been examined whether Poly $(A)_{20}$ RNA had an effect on binding of initiation factors to PK1 RNA. Fluorescence anisotropy measurements for binding of 5` fluorescein tagged PK1 RNA with initiation factors alone and in the protein complex form in the presence of Poly$(A)_{20}$ were studied. 50nM PK1 RNA was titrated with eIF4F·Poly $(A)_{20}$, eIF4B·Poly $(A)_{20}$, PABP·Poly$(A)_{20}$, eIF4F·eIF4B·Poly$(A)_{20}$, eIF4F·PABP·Poly$(A)_{20,}$ or eIF4F·eIF4B·PABP·Poly$(A)_{20.}$

Poly (A) enhances eIF4F, eIF4B, and PABP binding to PK1 RNA- The effect of Poly $(A)_{20}$ on individual initiation factors , eIF4F, eIF4B, and PABP, binding to PK1 RNA was studied. Addition of Poly $(A)_{20}$ to eIF4F showed a slight enhancement on the binding to PK1. K_d for eIF4F and eIF4F·Poly$(A)_{20}$ binding to PK1 RNA (Fig 13) was 203 ± 14 and 154 ± 11 nM, respectively. While addition of Poly $(A)_{20}$ to eIF4B (Fig 14) showed 1.4 fold tighter binding to PK1 RNA , PABP·Poly$(A)_{20}$ (Fig 15) showed 1.6 fold better binding to PK1. K_d for eIF4B and eIF4B·$(A)_{20}$ binding to PK1 RNA was 1383 ± 93 and 996 ± 77 nM, respectively. K_d for PABP and PABP·$(A)_{20}$ binding to PK1 RNA was 1765 ± 99 and 1169 ± 71 nM, respectively.

Poly (A) enhances eIF4F·4B binding to PK1 RNA-Addition of Poly $(A)_{20}$ to eIF4F·4B complex resulted with a better binding to PK1. Poly (A) increased eIF4F·4B binding to PK1 1.7 fold. While K_d of eIF4F·4B binding to PK1 RNA is 95 ± 5, K_d of eIF4F·4B· Poly $(A)_{20}$ is 57 ± 3.7 nM. Figure 16 shows binding of the eIF4F·4B protein complex to PK1 RNA in the presence and absence of Poly$(A)_{20}$ at 25°C . The binding measurements were carried out also at different temperatures, 15 °C, 10 °C, and 5 °C (Table 4).

Poly (A) enhances eIF4F·PABP binding to PK1 RNA- It was reported that eIF4F·PABP or eIF(iso)4F·PABP complexes show a 40 fold enhancement of cap analogue binding as compared to eIF4F or eIF(iso)4F alone. Here, we investigated effect of Poly (A) on the binding of eIF4F·PABP to PK1 RNA. The results showed that Poly(A) enhanced the affinity of eIF4F·PABP to PK1; eIF4F·PABP· Poly $(A)_{20}$ bound to PK1 4 fold more strongly than did eIF4F·PABP. K_d for eIF4F·PABP and eIF4F·PABP· Poly $(A)_{20}$ binding to PK1 RNA was 113 ± 9 and 29 ± 3.3 nM, respectively. Figure 17 shows binding of the protein complex to PK1 RNA in the presence and absence of Poly(A). Titration data for binding of eIF4F·PABP· Poly $(A)_{20}$ to the PK1 RNA at different temperatures ,15 °C, 10 °C, and 5 °C, are shown in Table 4.

Poly (A) stimulates eIF4F·eIF4B·PABP binding to PK1 RNA- We investigated whether association of Poly(A) with eIF4F·eIF4B·PABP protein complex affects binding activity of the complex to PK1 RNA. Titration of PK1 RNA with eIF4F·eIF4B·PABP· Poly $(A)_{20}$ complex showed that Poly(A) enhanced the affinity of protein complex to PK1; eIF4F·eIF4B·PABP· Poly$(A)_{20}$ bound to PK1 about 3 fold more strongly than did eIF4F·eIF4B·PABP (Table 4). K_d for eIF4F·eIF4B·PABP and eIF4F·eIF4B·PABP· Poly $(A)_{20}$ binding to PK1 RNA was 51 ± 2.5 and 18.3 ± 1.9 nM, respectively. Figure 18 shows binding of the protein complex to PK1 RNA in the presence and absence of Poly(A). Tabulated results of binding data of eIF4F·eIF4B·PABP·Poly$(A)_{20}$ to the PK1 RNA at different temperatures 15 °C, 10 °C, and 5 °C, are shown in Table 4.

A Van't Hoff plot of ln K_{eq} versus the reciprocal of temperature (1/T) was used to calculate the thermodynamic parameters of enthalpy (ΔH) and entropy (ΔS) for the interactions of initiation factors in presence of Poly$(A)_{20}$ with PK1 RNA (Fig. 19). The values of ΔH and ΔS were obtained from the slope and intercept, respectively (Table 5). The ΔG values at 25 °C were calculated from equation 3. The van't Hoff analyses showed that the PK1 RNA binding to eIF4F·4B and eIF4F·PABP in the presence of Poly$(A)_{20}$ are both enthalpy and entropy-favorable. This suggests hydrophobic interactions may play a role in binding. This may happen either directly from interactions with the RNA or through conformational changes in the protein. Addition of eIF4B·PABP·Poly$(A)_{20}$ complex to eIF4F caused the very dramatic change in the entropic contribution (ΔS = 21.9 ± 1.4 as compared to 76.0 ± 3.6) for PK1

binding. Overall, formation of protein complex favors hydrophobic interactions and RNA binding is primarily enthalpic that implies that hydrogen bonds are involved.

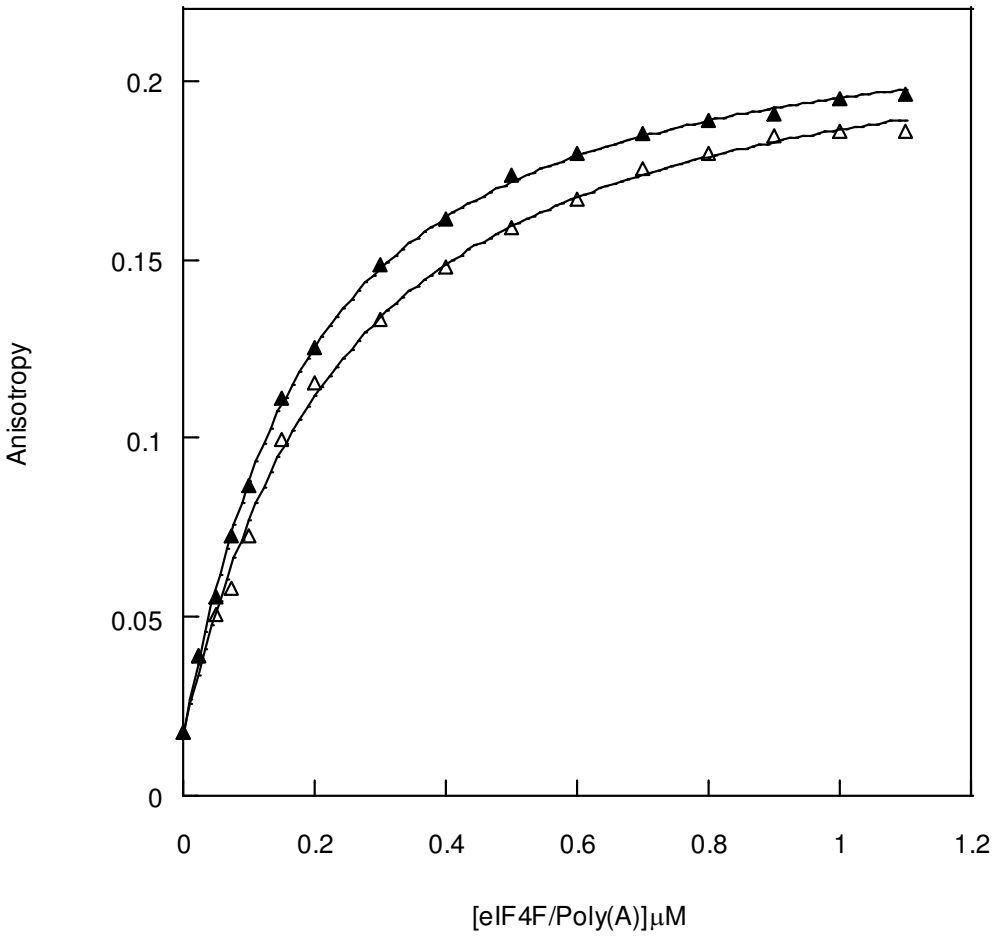

Figure 13.Fluorescence anisotropy measurements for the binding of fluorescein tagged PK1 RNA with translation initiation factors. The anisotropy values of eIF4F (—Δ—) and eIF4F·Poly(A)$_{20}$ (—▲—) are shown. The fluorescein tag PK1 RNA concentration was 50 nM in Titration Buffer at 25 °C. The excitation and emission wavelengths were 490 nm and 519 nm, respectively.

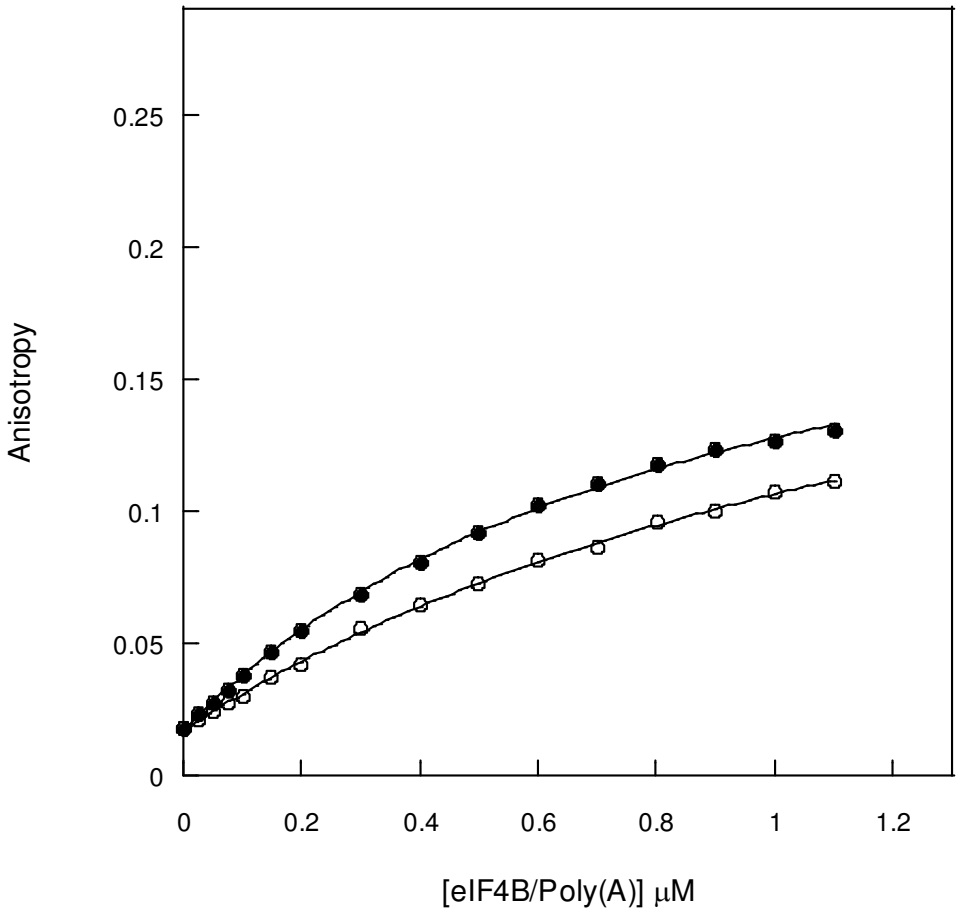

Figure 14.Fluorescence anisotropy measurements for the binding of fluorescein tagged PK1 RNA with translation initiation factors. The anisotropy values of eIF4B (—O—) and eIF4B·Poly(A)$_{20}$ (—•—) are shown. The fluorescein tag PK1 RNA concentration was 50 nM in Titration Buffer at 25 °C. The excitation and emission wavelengths were 490 nm and 519 nm, respectively.

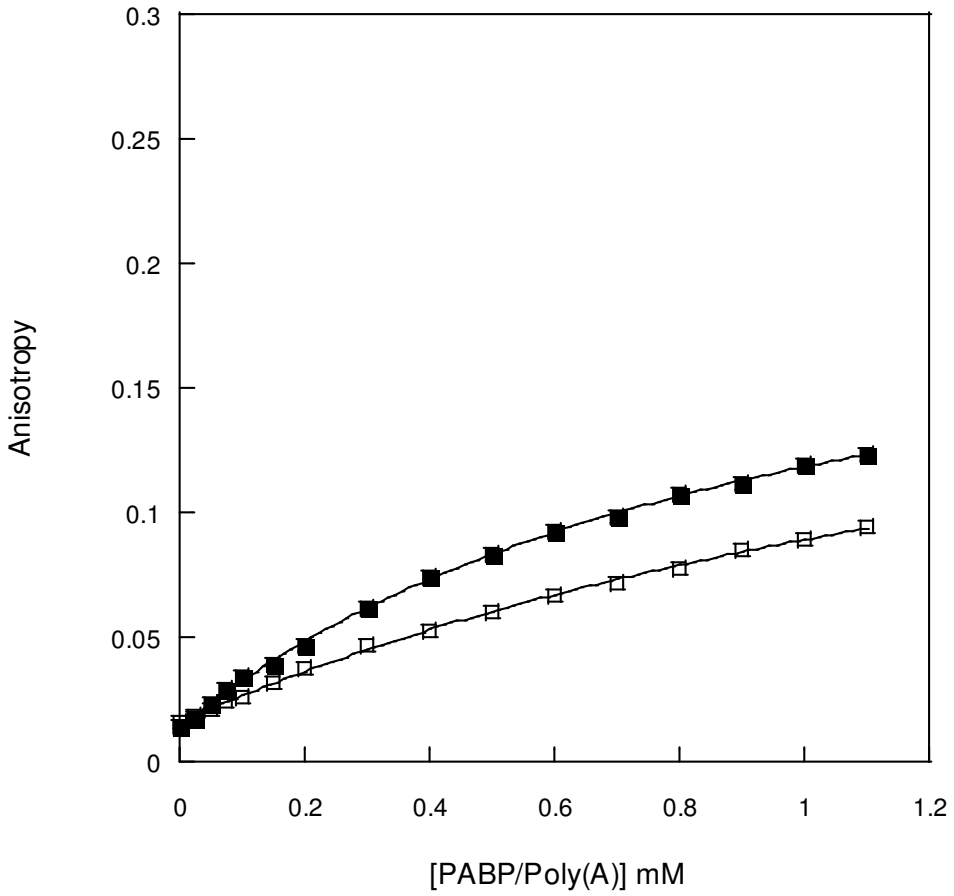

Figure15.Fluorescence anisotropy measurements for the binding of fluorescein tagged PK1 RNA with translation initiation factors. The anisotropy values of PABP (—□—) and PABP·Poly(A)$_{20}$ (—■—) are shown. The fluorescein tag PK1 RNA concentration was 50 nM in Titration Buffer at 25 °C. The excitation and emission wavelengths were 490 nm and 519 nm, respectively.

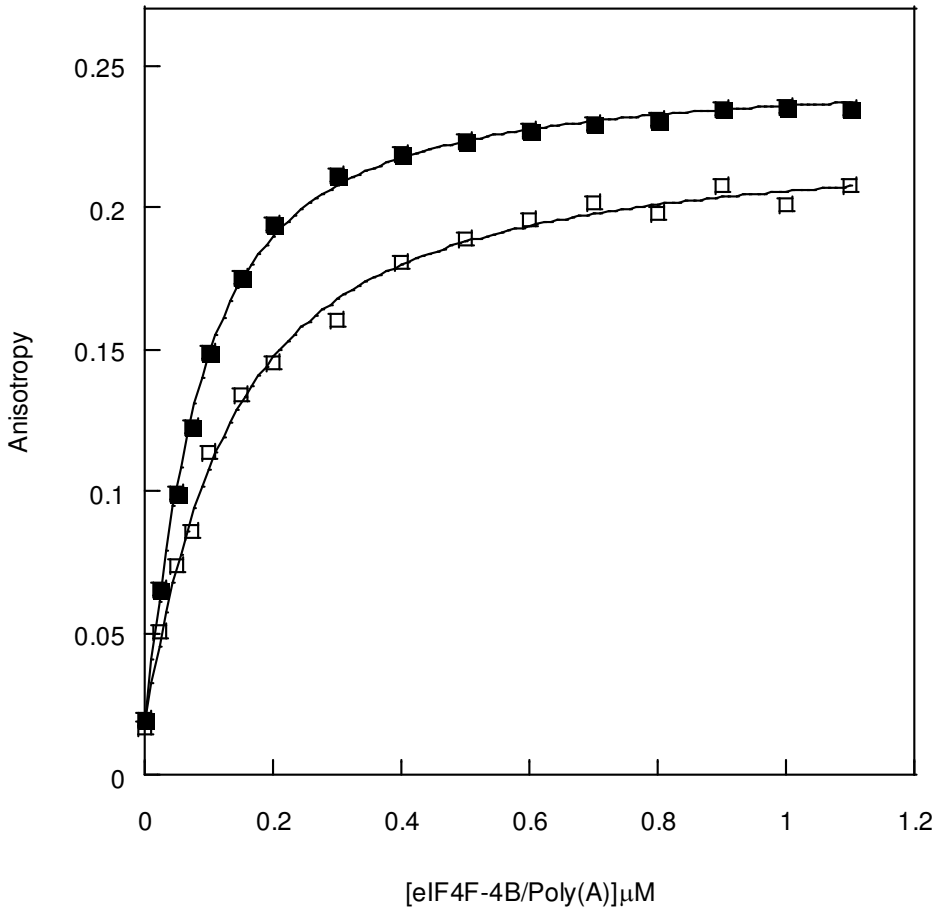

Figure 16. Fluorescence anisotropy measurements for the binding of fluorescein tagged PK1 RNA with translation initiation factors. The anisotropy values of eIF4F·4B (—□—) and eIF4F·4B·Poly$(A)_{20}$ (—■—) are shown. The fluorescein tag PK1 RNA concentration was 50 nM in Titration Buffer at 25 °C. The excitation and emission wavelengths were 490 nm and 519 nm, respectively. The solid lines are the fitted curves. eIF4F·eIF4B·Poly $(A)_{20}$ complex were prepared by incubation of 1 μM of eIF4F·eIF4B and 10 μM of Poly $(A)_{20}$ for 15 min at 4 °C and 90 % of the Poly $(A)_{20}$ was associated in the complex form at 50 nM titration concentration.

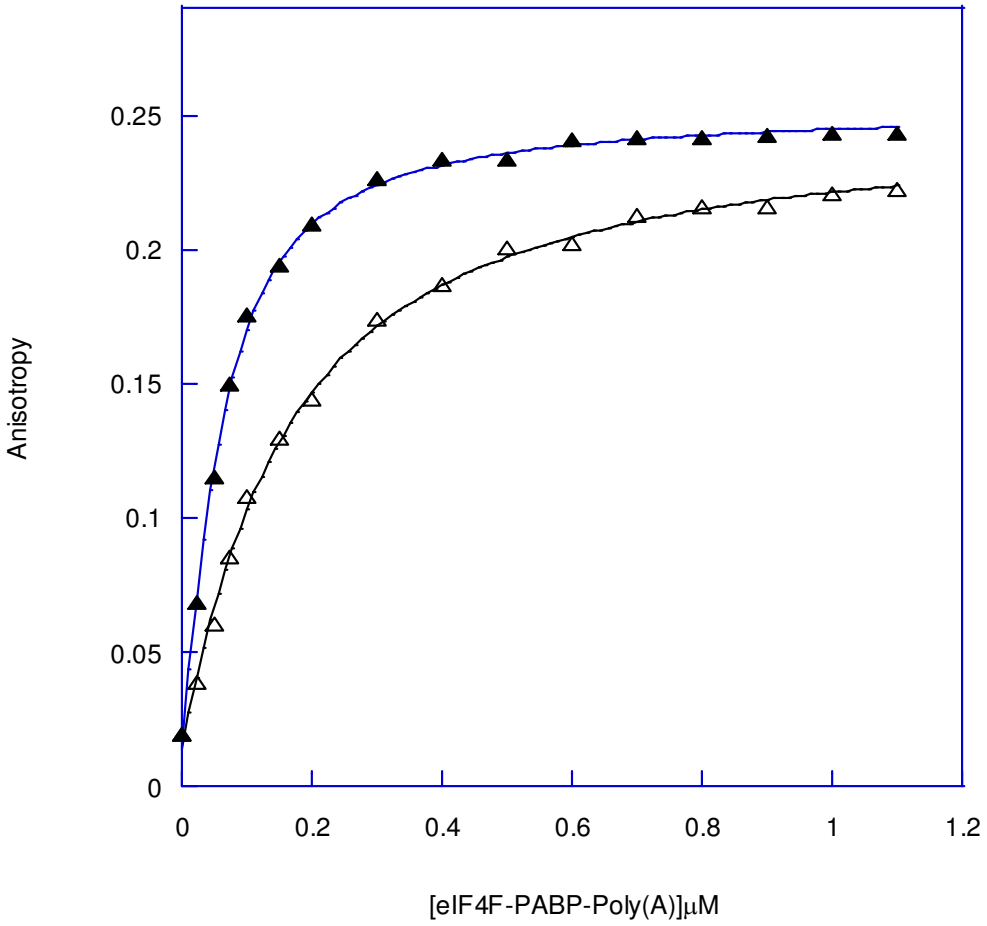

Figure 17. Fluorescence anisotropy measurements for the binding of fluorescein tagged PK1 RNA with translation initiation factors. The anisotropy values of eIF4F·PABP (—Δ—) and eIF4F·PABP· Poly $(A)_{20}$ (—▲—) are shown. The fluorescein tag PK1 RNA concentration was 50 nM in Titration Buffer at 25 °C. The excitation and emission wavelengths were 490 nm and 519 nm, respectively. The solid lines are the fitted curves. eIF4F·PABP·Poly $(A)_{20}$ complex were prepared by incubation of 1 µM of eIF4F·PABP and 5 µM of Poly $(A)_{20}$ for 15 min at 4 °C and 90 % of the Poly $(A)_{20}$ was associated in the complex form at 50 nM titration concentration.

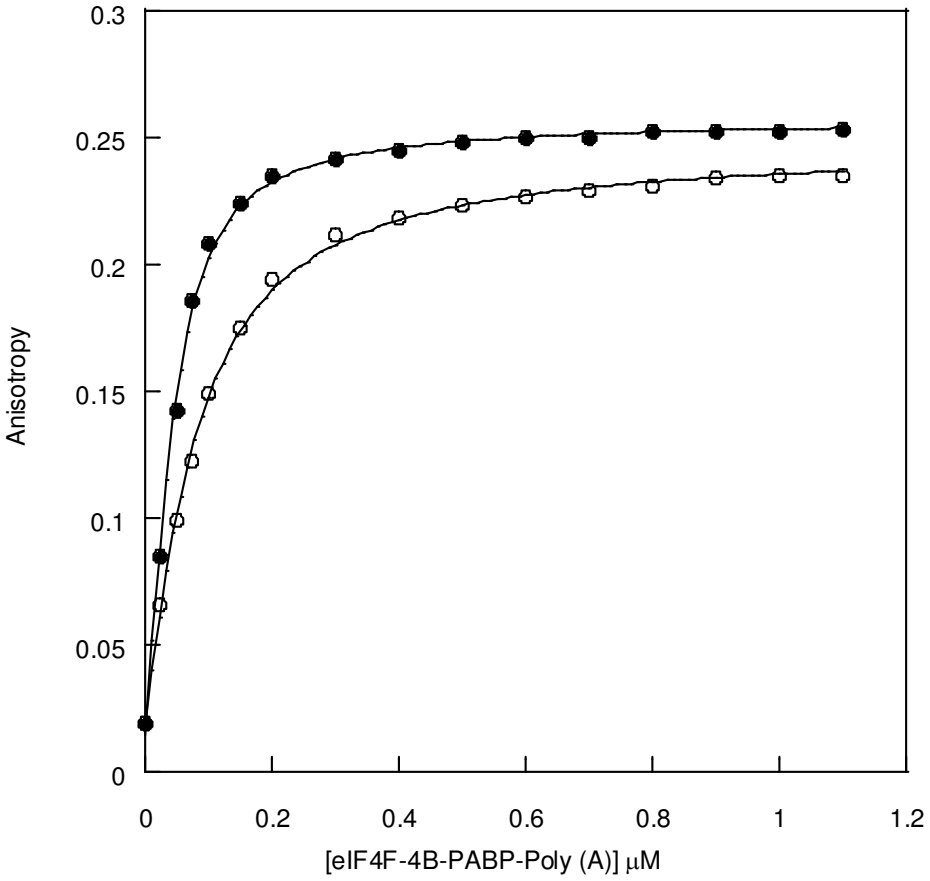

Figure 18. Fluorescence anisotropy measurements for the binding of fluorescein tagged PK1 RNA with translation initiation factors. The anisotropy values of eIF4F·eIF4B·PABP(—O—),and eIF4F·eIF4B·PABP· Poly $(A)_{20}$ (—•—) are shown. The fluorescein tag PK1 RNA concentration was 50 nM in Titration Buffer at 25 °C. The excitation and emission wavelengths were 490 nm and 519 nm, respectively. The solid lines are the fitted curves. eIF4F·eIF4B·PABP·Poly $(A)_{20}$ complex were prepared by incubation of 1 μM of eIF4F·eIF4B·PABP and 6 μM of Poly $(A)_{20}$ for 15 min at 4 °C and 95 % of the Poly $(A)_{20}$ was associated in the complex form at 50 nM titration concentration.

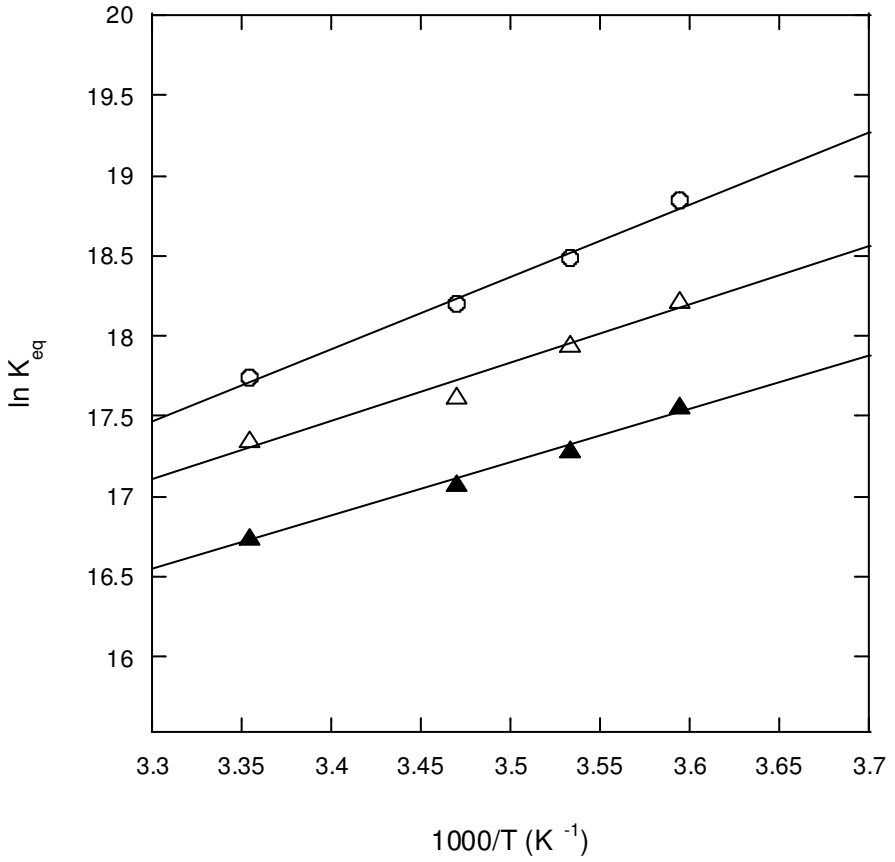

Figure 19.Van't Hoff plots for the interaction of ^{FI}PK1 RNA with translation initiation factors in the presence of Poly $(A)_{20}$. The data are indicated as eIF4F·eIF4B·PABP·Poly $(A)_{20}$-PK1 (—O—), eIF4F·PABP·Poly$(A)_{20}$-PK1 (—Δ—) and eIF4F·4B·Poly$(A)_{20}$-PK1 (—▲—).Enthalpy (ΔH) and entropy (ΔS) were calculated from the slope and intercept of the temperature dependent equilibrium binding measurements, respectively.

Table 4. Equilibrium dissociation constants (K_d) for the interaction of eIF4F·4B·PABP· Poly $(A)_{20}$,eIF4F·PABP· Poly $(A)_{20}$,eIF4F·4B· Poly $(A)_{20,}$ eIF4F· Poly $(A)_{20}$, eIF4B · Poly $(A)_{20}$ and PABP· Poly $(A)_{20}$ with fluorescein tag PK1 RNA (^{FI}PK1).

Complex	PK1 25 ºC (K_d nM)	PK1 15 ºC (K_d nM)	PK1 10 ºC (K_d nM)	PK1 5 ºC (K_d nM)
eIF4F·4B·PABP·Poly $(A)_{20}$-PK1	18.3 ± 1.9	13 ± 1.5	9.8 ± 0.7	7 ± 0.4
eIF4F·PABP·Poly $(A)_{20}$-PK1	29 ± 3.3	22 ± 2.6	16 ± 1.4	12 ± 1.2
eIF4F·4B·Poly $(A)_{20}$-PK1	57 ± 3.7	42.8 ± 3.3	36.8 ± 2.9	28.2 ± 2
eIF4F·Poly $(A)_{20}$-PK1	154 ± 11			
eIF4B·Poly $(A)_{20}$ -PK1	996 ± 77			
PABP·Poly $(A)_{20}$-PK1	1169 ± 71			

Table 5. Thermodynamic parameters of enthalpy, entropy and free energy change for the interactions of eukaryotic initiation factors in the presence of Poly(A)$_{20}$ complex with ^{FI}PK1 RNA.

Complex	ΔH (kJ mol^{-1})	ΔS (J mol^{-1}K^{-1})	ΔG (kJ mol^{-1})
eIF4F·4B·Poly(A)$_{20}$ -PK1	-27.77 ± 1.1	45.87 ± 2.6	-41.45
eIF4F·PABP·Poly(A)$_{20}$ -PK1	-30.22 ± 1.7	42.48 ± 2.1	-42.87
eIF4F·4B·PABP Poly(A)$_{20}$ PK1	-37.36 ±1.3	21.9 ± 1.4	-43.9

3.6 Kinetics of eIF4F and eIF4F·4B Binding to ^{FI}PK1

Following fluorescence titration studies, kinetics of eIF4F and eIF4F·4B binding to ^{FI}PK1 were studied. First, the rates of eIF4F binding to PK1 were studied. Then, the effect of addition of eIF4B on the rate of binding of eIF4F to PK1 was measured. The stopped-flow data were plotted as the anisotropy *versus* time as shown in figures. A single-exponential equation provided the best fit to the data over the entire time course of measurements. eIF4F and eIF4F·4B proteins were rapidly mixed with PK1 RNA in the stopped flow instrument at 25 °C as shown in Figure 20. k_{obs} values for eIF4F and eIF4F·4B binding to PK1 RNA were $k_{obs} = 57.2 \pm 2.3$ s^{-} and 103 ± 4.8 s^{-1}, respectively. These results demonstrate that binding of eIF4F·4B showed about 2-fold higher k_{obs} rate constant than eIF4F binding to PK1 RNA. Applying double exponential function to the data did not improve the fit (data not shown).

Subsequently, protein concentration dependence of PK1 RNA with eIF4F and eIF4F·4B were studied. Stopped-flow anisotropy of PK1 RNA (50 nM) with varying concentration (0.1 to 1 μM) of eIF4F and eIF4F·4B was acquired.

The mechanism of the reaction is one step, pseudo-first order reaction,

$$\text{eIF4F} + \text{PK1} \underset{k_{off}}{\overset{k_{on}}{\rightleftharpoons}} \text{eIF4F/ -PK1}$$

where k_{on} is rate of association and k_{off} is rate of dissociation constant.

The observed rate constant, k_{obs}, is predicted to be a linear function of the concentration of eIF4F (Eq 6).

$$k_{obs} = k_{on}\,[\text{eIF4F}] + k_{off} \qquad \text{(Eq 6)}$$

Increasing of protein concentrations resulted in an increase in anisotropy of RNA (Fig 21 and Fig 22). Further, k_{obs} increased linearly with an increase of protein concentration (Fig 23). k_{on} and k_{off} values were obtained from the slope and the y-intercept, respectively. These data are shown in Table 6. The k_{on} and $k_{off\ values}$ for eIF4F-PK1 were 55 + 2 $\mu M^{-1}\ s^{-1}$ and 11.6 + 0.3 s^{-1}, respectively. The same stopped flow experiments were performed for PK1 RNA (50nM) with varying concentration (0.1 to 1 μM) of eIF4F·4B. Similar to eIF4F binding to PK1 RNA, k_{obs} for eIF4F·4B interaction with PK1 RNA increased linearly with an increase of eIF4F·4B concentration (Fig 24). The k_{on} and k_{off} values for eIF4F·4B-PK1 were 94.1 ± 4.3 $\mu M^{-1}\ s^{-1}$ and 10.2 ± 0.7 s^{-1}, respectively. The k_{on}

of eIF4F·4B-PK1 is about 2 fold greater than k_{on} of eIF4F-PK1. Using k_{on} and k_{off} values K_d values were calculated according to Eq 7:

$$K_d = k_{off}/k_{on} \qquad \text{(Eq7)}$$

The calculated K_d values are 212 nM for eIF4F and 108 nM for IF4F·4B with PK1 RNA. The results show that the eIF4F·4B complex has about 2 fold higher affinity than eIF4F to PK1 RNA (Table 6). These results are consistent with the results obtained from fluorescence steady state experiments that revealed that eIF4F·4B complex has 2 fold greater affinities to PK1 than affinity of eIF4F to PK1 RNA. K_d values calculated from the kinetic constant agree well with the K_d value obtained by steady state equilibrium method (Table 6).

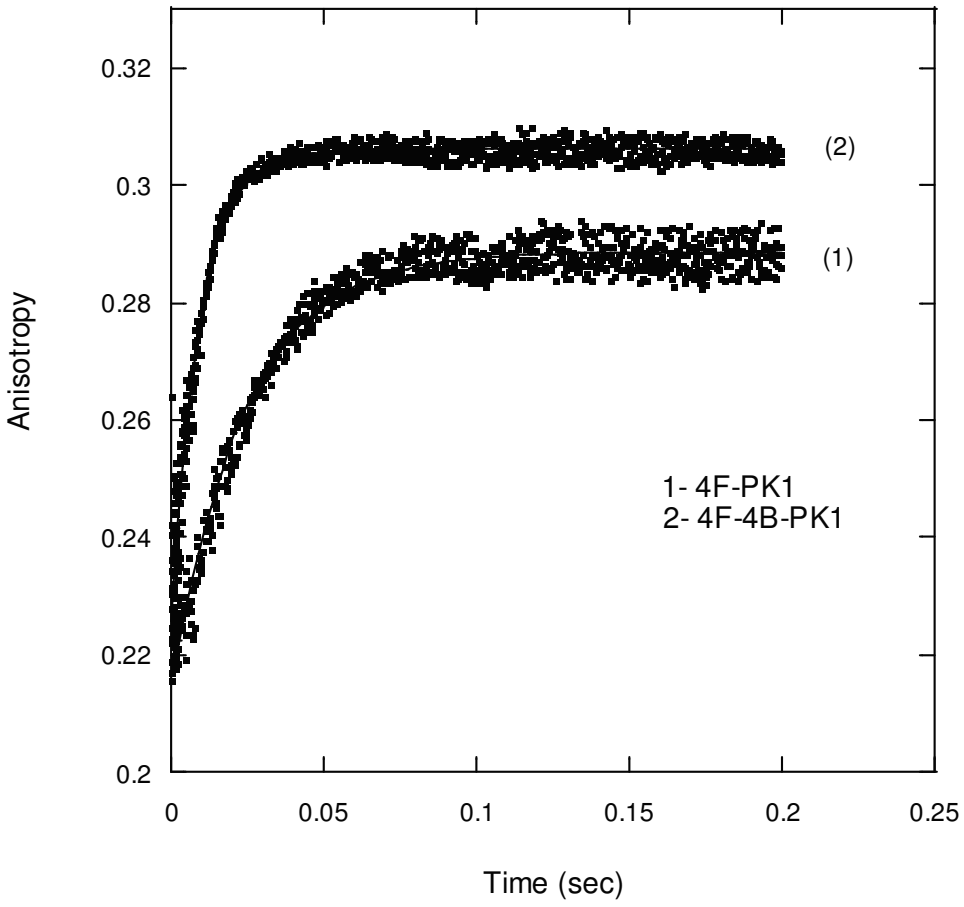

Figure 20. Kinetic analysis for the PK1 RNA binding to eIF4F and eIF4F·4B measured by stopped-flow anisotropy. FIuorescein-labeled PK1 RNA at 50 nM (final concentration) was rapidly mixed with 1000 nM eIFs (final concentration) at 25 °C. The data were fit to a single-exponential fits to the fluorescence anisotropy data.

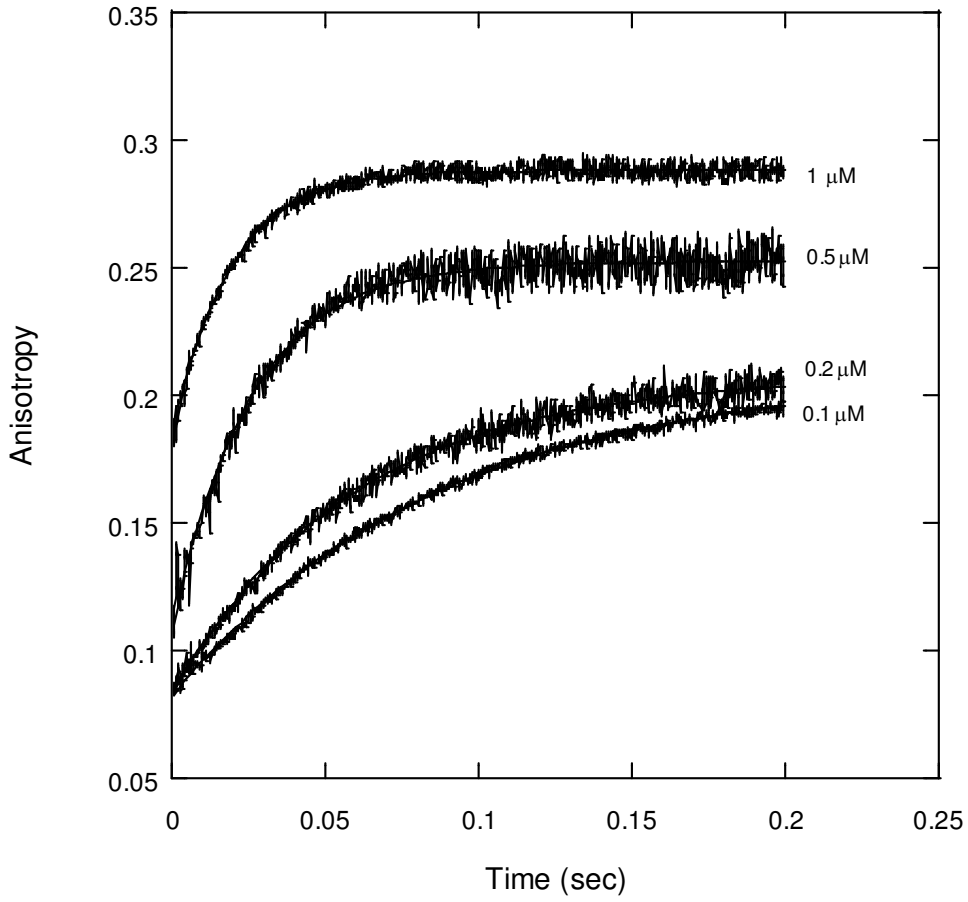

Figure 21. Kinetics of eIF4F induced anisotropy change in PK1 RNA binding. ^{FI}PK1 RNA at 50 nM was rapidly mixed with varying concentrations (0.1, 0.2, 0.5 and 1 μM, final) of eIF4F at 25 °C. The resulting time course of anisotropy change that fits to a single-exponential function at different concentration with k_{obs} of 15, 17.0, 33, and 57 s^{-1}, respectively.

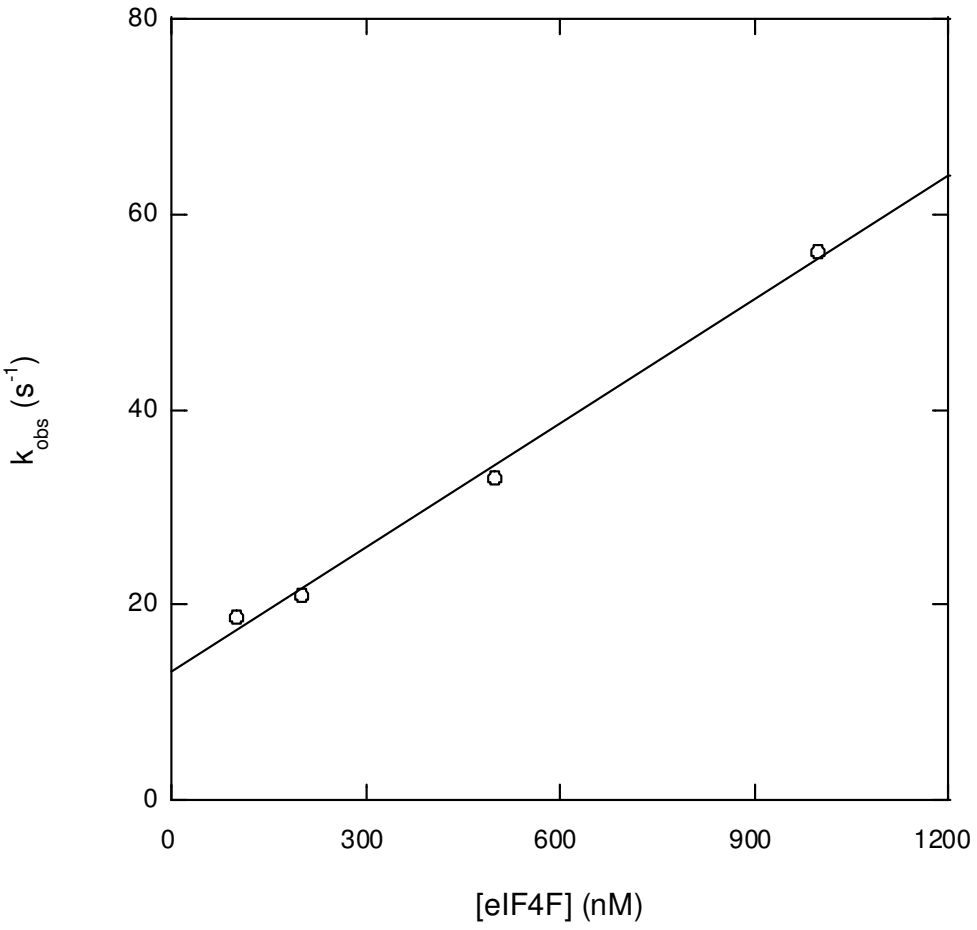

Figure 22. Kinetics of eIF4F induced anisotropy change in PK1 RNA binding. ^{FI}PK1 RNA at 50 nM was rapidly mixed with varying concentrations (0.1, 0.2, 0.5 and 1 μM, final) of eIF4F at 25 °C. The observed rate constant of anisotropy change, 15, 17.0, 33, and 57 s^{-1} , is plotted as a function of increasing eIF4F concentrations that provide a k_{on} of 54.8 ± 2.1 $\mu M^{-1}s^{-1}$.

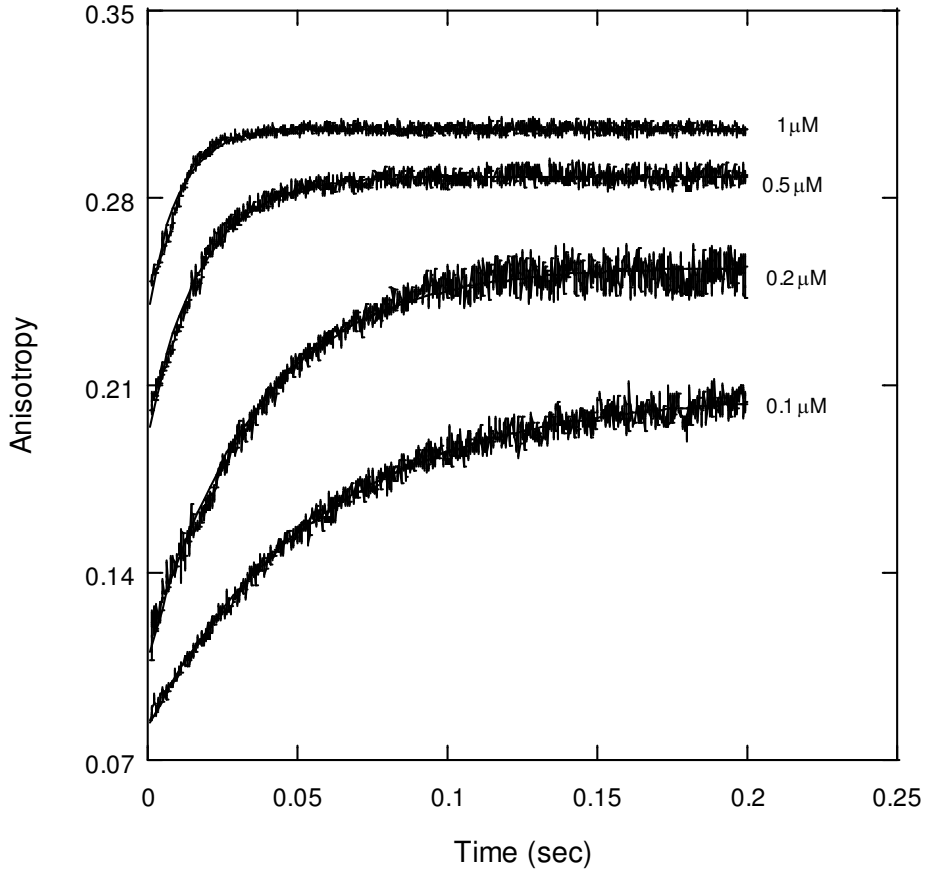

Figure 23. Rate of eIF4F·4B induced anisotropy change in PK1 RNA binding. ^{FI}PK1 RNA at 50 nM was rapidly mixed with varying concentrations of eIF4F·4B (0.1, 0.2, 0.5 and 1 μM, final) at 25 °C. The resulting time course of anisotropy change that fits to a single-exponential function at different concentrations with k_{obs} of 23, 31, 61 and 103 s^{-1}, respectively.

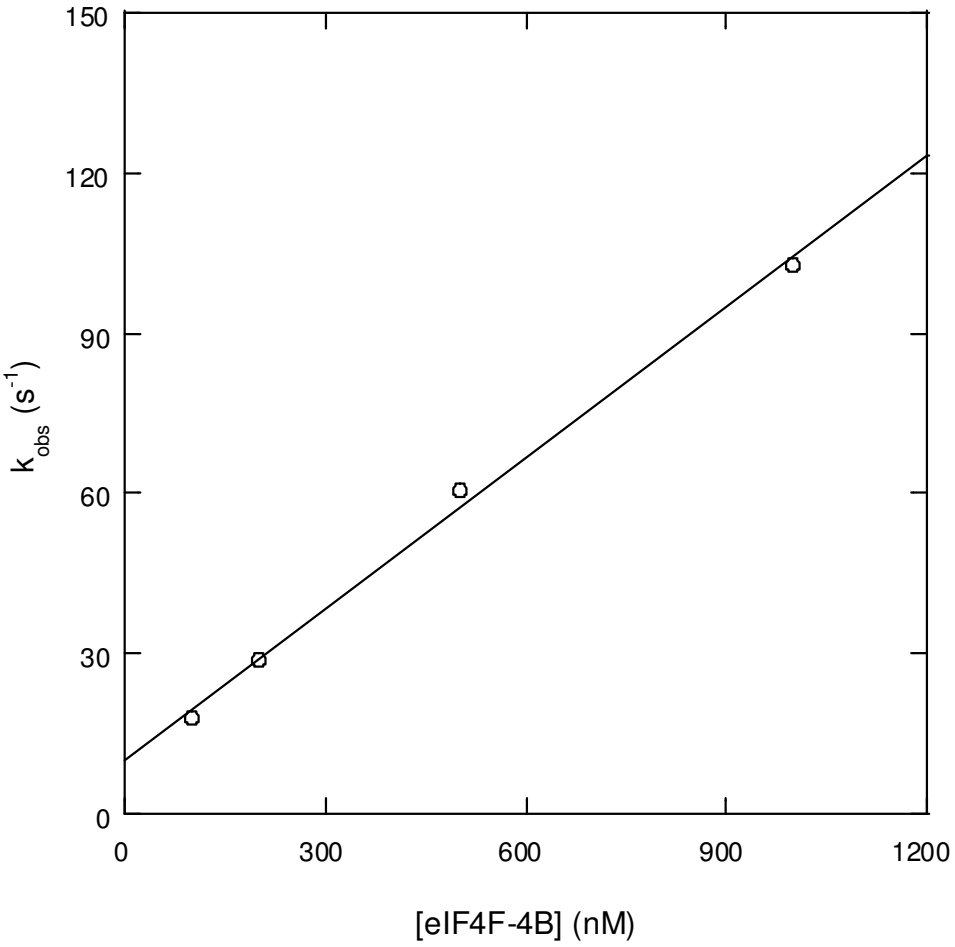

Figure 24. Kinetics of eIF4F·4B induced anisotropy change in PK1 RNA binding. ^{FI}PK1 RNA at 50 nM was rapidly mixed with varying concentrations of eIF4F·4B, 0.1, 0.2, 0.5 and 1 μM, at 25 °C. The observed rate constant of anisotropy change, 23, 31, 61 and 103 s^{-1}, is plotted as a function of increasing eIF4F·4B concentrations that provide a k_{on} of 94.1 ± 4.3 $\mu M^{-1}s^{-1}$

Table 6. Kinetic parameters for the binding of PK1 RNA with eIF4F and eIF4F·4B complex.

Complex	k_{on} ($\mu M^{-1} s^{-1}$)	k_{off} (s^{-1})	k_{off}/ k_{on} (nM)	K_d (Steady state)[a] (nM)
eIF4F-PK1	55 ± 2	11.6 ± 0.3	212	203 ± 14
eIF4F·4B-PK1	94.1 ± 4.3	10.2 ± 0.7	108	95 ± 5

[a]Determined by steady state fluorescence method.

4.0 Discussion

Picornaviral mRNAs are polyadenylated and employ cap-independent translation initiation. Zeenko and Gallie (19) showed that TEV 5'-leader functionally substitutes for a 5'-cap and promotes cap-independent translation through a 49-nucleotide pseudoknot containing domain, PK1. PK1 contains nucleotide sequence complementary to a highly conserved region of 18 S RNA. Mutational studies (19) showed that any mutation on this complementary sequence caused disruption of cap-independent translation.

Previous studies (46,50) demonstrated that wheat germ poly(A)-binding protein (PABP) interacted with eIFiso4G and eIF4B and the interaction of eIF4F, eIF4B, or eIFiso4F with PABP enhances the binding affinity for Poly (A) RNA (46). Further, eIFiso4F·PABP or eIF4F·PABP complexes are shown to increase the binding affinity to the 5'-cap analogues by 40-fold and promote the ATPase and RNA helicase activity of the eIF4F·eIF4A·eIF4B complex (60,50). It has been demonstrated that PABP aids the stable recruitment of eIF4F to an mRNA by increasing its binding affinity to 5'-cap and decreasing its dissociation from the 5'-cap (41,42). We have reported that PK1 interacts with eIF4F and showed the first quantitative information on the binding interactions of plant translation initiation factors with an IRES and demonstrated that the TEV leader can distinguish between

eIF4F isoforms to preferentially recruit one isoform over the other (20). We recently determined the effects of eIF4B and PABP on these interactions. Addition of PABP and eIF4B increased the binding affinity of eIF4F by 4-fold for PK1 RNA as compared with eIF4F alone. These data show that the effect of eIF4B and PABP on PK1 RNA binding is much more moderate as compared to their effect on cap binding where 40-fold enhancement was observed. By binding 5' cap and the 3' Poly(A) tail, eIF4F-PABP complex induces a circular structure on the capped mRNA (closed loop), which assists ribosome re-entry. Having a relatively small contribution from PABP on uncapped PK1 binding suggests that tobacco etch virus may not undergo PABP imposed circularization of mRNA and PABP is less important for initiation complex. However, even though eIF4B and PABP did not show the effect they produced in cap binding, K_d of PK1, even for eIF4F alone, is substantially tighter than cap binding (0.203 µM compared to 8.9µM).

There are certainly a number of proteins, such as NSP3 protein, unrelated to PABP, capable of interacting with viral 3` end and involve in IRES mediated translation. It has been shown that Poly(A) stimulation is susceptible to the addition of the rotaviral NSP3 protein(61). Although NSP3 and PABP do not possess any similarity in primary or tertiary structure, mutagenesis and binding experiments specify that both proteins bind the same surface of eIF4G by similar mechanisms, NSP3 showing the higher affinity, and NSP3 competitively displaces PABP from eIF4G. One other

possible explanation of PABP having less impact on IRES binding is that NSP3 may substitute for PABP and assist viral RNA circularization.

Both the 5' cap and the poly (A) tail of eukaryotic mRNAs are important regulators of translation efficiency. The 5'-cap and the poly(A) tail act synergistically to increase the translational efficiency of eukaryotic mRNAs, which suggests that these two mRNA elements communicate during translation. We showed that in the presence of $Poly(A)_{20,}$ eIF4F·PABP bound to PK1 about 4-fold tighter. Further, the addition of $Poly(A)_{20}$ to eIF4F·eIF4B·PABP complex caused a tighter binding to uncapped PK1 RNA. The equilibrium dissociation constant of the complex binding to PK1 RNA decreased from 51 ± 2.5 nM to 18.3 ± 1.9 nM in the presence of $Poly(A)_{20.}$ Addition of Poly $(A)_{20}$ increases the binding affinity of eIF4F·eIF4B·PABP complex by about 3-fold for PK1 RNA. Overall, eIF4F·eIF4B·PABP·$Poly(A)_{20}$ complex has 11-fold higher affinity to PK1 RNA as compared with binding affinity of eIF4F alone. While addition of both eIF4B and PABP to eIF4F caused 4 fold tighter binding to PK1, addition of only Poly $(A)_{20}$ to the eIF4F·eIF4B·PABP complex caused 3 fold better binding.

Thermodynamic studies showed that eIF4F binding to PK1 in the presence of eIF4B, PABP, and $Poly(A)_{20}$ has significantly less entropic contribution. The relatively small entropic contributions to the protein

complex of eIF4F·eIF4B·PABP and Poly(A)$_{20}$ to PK1 RNA suggest that hydrophobic residues are more solvent exposed in the combined structure. This implies that hydrogen bonds are involved. Therefore, it does not seem to be a large conformational change takes place during eIF4F binding to PK1.

Using stopped-flow anisotropy, we also investigated kinetics of PK1 RNA binding to eIF4F and eIF4F·4B. The values of k_{on} obtained from the observed rates, which are acquired from the concentration dependence experiments. Almost 2 fold difference k_{on} rate constant was observed for eIF4F·4B (k_{on} = 94.1 ± 4.3 μM^{-1} s^{-1}) binding to PK1 RNA as compared to eIF4F (k_{on} = 54.8 ± 2.1 $\mu M^{-1}s^{-1}$) binding to PK1 RNA. Table 6 shows on rate (k_{on}) and the dissociation rate constant (k_{off}) for eIF4F and eIF4F·4B. eIF4F-PK1 RNA complex shows a slower rate of dissociation in the presence of eIF4B (k_{off} = 10.2 ± 0.7 s^{-1} for eIF4F·4B; k_{off} = 11.6 ± 0.3 s^{-1} for eIF4F). This data shows the binding of PK1 RNA to eIF4F is highly kinetically favored and a more stable complex in the presence of eIF4B suggests a pathway for assembly of a complex for protein synthesis initiation. The kinetic effect of eIF4B on binding affinity eIF4F to PK1 RNA must reside mainly in the dissociation rates. eIF4F·4B complex binds PK1 RNA with higher rate than eIF4F and will be able to form a more stable intermediate with rapid binding to PK1 RNA and should significantly increase the rate of protein synthesis. Association of eIF4F with eIF4B presents a complex that has rapid binding and provides a lower rate of dissociation of the PK1 RNA to the complex.

These data provide further insights into the formation of the translation initiation complex of the tobacco etch virus. The information obtained from this research has potential use to develop systems to produce desired proteins, which are nutritionally beneficial and have other economic uses. Future studies involving binding interactions of the other initiation factors and proteins, such as NSP3, will give more information about the mechanism of cap independent translation of TEV.

APPENDIX

1.1 Cell media

1L Luria-Bertani (LB) media

Yeast Extract	5g
Peptone	10g
NaCl	10g
ddH_2O	1000ml

1.2 Buffers for Electrophoresis

For DNA Agarose Gel

50xTAE buffer pH 8.0

Tris Base	242g
EDTA	18.6g
Glacial Acetic Acid	57.1g
ddH_2O	to 1000ml

6x DNA sample loading buffer

Bromophenol Blue	0.5ml
1.0% Glycerol	4.0ml
50x TAE buffer	0.2ml
ddH_2O	to 10 ml

For Protein Gel

10x Tank buffer pH 8.8

Tris Base	24.22g
SDS	10g
Glycine	144.40g
ddH_2O	to 1000ml

6x Protein Sample Loading buffer

4x Stacking Gel buffer	1.56ml
SDS	1.0g
Glycerol	5.0ml
Bromphenol blue	0.5ml
1.0% β-mercaptoethanol	2.5ml
ddH_2O	to 10 ml

4x Resolving Gel buffer (1M Tris-Cl buffer pH8.8)

4x Stacking Gel buffer (0.5M Tris-Cl buffer pH6.8)

1.3 Determine the protein concentration by Bradford Method

The Bradford method to determine protein concentration is by the Coomassie® - Protein Reaction

Protein + Coomassie® G-250 in an acidic medium →protein-dye complex (blue color, measured at 595 nm)

The protocols used in this experiment are as following:

1. Preparation of Diluted BSA Standards

Prepare a fresh set of protein standards by diluting the 2.0 mg/ml BSA stock standard (Stock) (preferably in the same diluent as your samples) as illustrated in TableA.1a below. 1 ml 2.0 mg/ml BSA standard is sufficient to prepare a set of diluted standards for either working range.

Table A.: Preparation of the Diluted BSA Standards

Standard Test Tube or Plate Protocol, Working Range = 100 - 1500 µg/ml

Volume of the BSA	Volume of Diluent	Final BSA Concentration
300µl of (stock)	0µl	2,000µg/ml
375µl of (stock)	125µl	1,500µg/ml (A)
325µl of (stock)	325µl	1,000µg/ml (B)
175µl of (A)	175µl	750µg/ml (C)
325µl of (B)	325µl	500µg/ml (D)
325µl of (D)	325µl	250µg/ml (E)
325µl of (E)	325µl	125µg/ml (F)
100µl of (F)	400µl	25µg/ml (G)

2. Mixing of the Coomassie® Plus Protein Assay Reagent

Allow the Coomassie® Plus Reagent to come to room temperature. Mix the Coomassie® Plus Reagent solution just prior to use by gently inverting the bottle several times. Do not shake.

3. Reaction

Pipet 0.05 ml of each standard or unknown sample into an appropriately labeled UV cuvette. Use 0.05 ml of the diluent for the blank. Add 1.5 ml of the Coomassie® Plus Reagent to each tube, mix well.

4.Detection

Switch on the Cary UV linked computer. Open the [Concentration] program on the windows desktop. Measure the absorbance at 595 nm of blank and zero the Cary UV reading. Measure the absorbance at 595 nm of each cuvette. Prepare a standard curve by plotting the average corrected 595 nm reading for each BSA standard versus its concentration in μg/ml. Using the standard curve, determine the protein concentration for each unknown sample

1.4 SDS Polyacrylamide Gel Electrophoresis (SDS-PAGE)

Assembling gel apparatus according to manufacturer's instructions:

Make gel and pour in the chamber according to the following protocol.

Resolving Gels:

Gel concentration of 12% in 0.25 M Tris-HCl pH 8.8

Reagent	**Volume to make 5 ml**	**Volume to make 10ml**
30% Acrylamide stock*	2.0ml	4.0ml
ddH_2O	1.5ml	3.2ml
1M tris-HCl pH8.8	1.3ml	2.5ml
10%SDS	0.1ml	0.2ml
Ammonium Persulphate	0.1ml	0.1ml
10%TEMED (added last)	1.5µl	1.5µl

*29:1 w:w ratio of acrylamide to N,N'-methylene bis-acrylamide

Mix ingredients very carefully in the order shown above, ensuring no air bubbles form. Pour into glass plate assembly. Overlay gel with isopropanol to ensure a flat surface and to exclude air. Wash off isopropanol with water after gel has polymerized (about15 min).

Stacking Gels:

Gel concentration of 5% in 0.125 M Tris-HCl pH 6.8

Reagent	**Volume to make 5ml**	**Volume to make 10 ml**
30% Acrylamide stock*	0.83ml	1.66ml
ddH_2O	2.72ml	5.54ml
0.5M Tris-HCl pH8.8	1.25ml	2.5ml
10%SDS	0.1ml	0.2ml
Ammonium Persulphate	0.1ml	0.1ml
10%TEMED (added last)	5µl	5µl

Mix as before, then pour onto top of set resolving gel, insert comb, allow to polymerize (about 30 minutes), remove comb, fill with electrophoresis buffer. Assemble top tank onto glass plate assembly. Fill with electrophoresis buffer.

Electrophoresis buffer

The final Tank buffer composition is 196mM glycine / 0.1% SDS / 50mM Tris-HCl pH 8.3, made by diluting a 10x stock solution. This goes in both top and bottom tanks.

The Protein samples:

Take supernatant and mix 50 µL 1:1 (v:v) with SDS-PAGE disruption mix: this is 125mM Tris-HCl pH 6.8 / 10% 2-mercaptoethanol / 10% SDS / 10% glycerol, containing a little bromophenol blue. For liquid / purified samples, take e.g. 100 µL and add 50 - 100 µL of disruption mix.

Heat sample tubes for 5 min at boiling water in a "float" in a water bath then keep on ice for 10 minutes. Layer samples under buffer into wells on stacking gels. Connect up apparatus electrophorese to the power supply. Set voltage as 150V and current as 20mA and run the gel until the blue dye reaches the bottom of the gel.

Stain the gel by using Coomassie Brilliant Blue R250

Stain: 0.2% Coomassie Brilliant Blue R250 in 45% 45% 10 % methanol water acetic acid. Cover gel with staining solution, seal in plastic box and leave overnight on shaker (RT) or for 2 to 3 hours at 37 °C also with agitation.

Destain with 25%/ 65%/ 10% methanol water acetic acid mix, with agitation. Change the distaining solution several times until the gel background color becomes transparent.

Bibliography

1. López-Lastra M, Rivas A, Barría MI, Protein synthesis in eukaryotes: the growing biological relevance of cap-independent translation initiation.

   Biol Res (2005), 38: 121-146,

2. Pestova TV, Kolupaeva VG, Lomakin IB, Pilipenko EV, Shatsky IN, Agol VI, Hellen CU., Molecular mechanisms of translation initiation in eukaryotes. Proc Natl Acad Sci U S A. (2001) June 19; 98(13): 7029–7036.

3. Merrick WC. Cap-dependent and cap-independent translation in eukaryotic systems. Gene. (2004) 332:1-11.

4. Kozak M., Rethinking some mechanisms invoked to explain translational regulation in eukaryotes, (2006) 382:1-11.

5. M.W. Hentze, eIF4G: a multipurpose ribosome adapter? Science (1997) 275:500–501

6. A.B. Sachs, P. Sarnow and M.W. Hentze, Starting at the beginning, middle, and end: translation initiation in eukaryotes, Cell 89 (1997), 831–838.

7. H. Le, R.L. Tanguay, M.L. Balasta, C.C. Wei, K.S. Browning, A.M. Metz, D.J. Goss and D.R. Gallie, Translation initiation factors eIF-iso4G and eIF-4B interact with the poly(A)-binding protein and increase its RNA binding activity, J. Biol. Chem. (1997) 272:16247–16255.

8. Jang, S.K., Krausslich, H.G., Nicklin, M.J., Duke, G.M., Palmenberg, A.C. and Wimmer, E. A segment of the 5' nontranslated region of encephalomyocarditis virus RNA directs internal entry of ribosomes during in vitro translation. J Virol, (1988) 62: 2636-43

9. Pelletier J, Sonenberg N Internal initiation of translation of eukaryotic mRNA directed by a sequence derived from poliovirus RNA, Nature (1988) 334: 320-5

10. Pestova TV, Hellen CU, Shatsky IN.,Canonical eukaryotic initiation factors determine initiation of translation by internal ribosomal entry, Mol Cell Biol. (1996) 12:6859-69.

11. Fernández-Miragall O, Martínez-Salas E Structural organization of a viral IRES depends on the integrity of the GNRA motif. RNA 9: 1333-44

12. Jang SK, Kräusslich HG, Nicklin MJ, Duke GM, Palmenberg AC, Wimmer E A segment of the 5' nontranslated region of encephalomyocarditis virus RNA directs internal entry of ribosomes during in vitro translation, J Virol (1988) 62: 2636-43

13. Martinez-Salas, E., Lopez de Quinto, S., Ramos, R. & Fernandez-Miragall, O IRES elements: Features of the RNA structure contributing to their activity. Biochimie (2002) 84: 755-63

14. Martínez-Salas E, Sáiz JC, Dávila M, Belsham GJ, Domingo E. A single nucleotide substitution in the internal ribosome entry site of foot-and-mouth

disease virus leads to enhanced cap-independent translation in vivo. J Virol (1993) 67: 3748-55

15. Pelletier J, Sonenberg N Internal initiation of translation of eukaryotic mRNA directed by a sequence derived from poliovirus RNA. Nature (1988) 334: 320-5

16. Holcik M., Lefebvre, C., Yeh, C., Chow, T. and Korneluk, R.G. A new internal-ribosome-entry-site motif potentiates XIAP-mediated cytoprotection, Nature Cell Biol. (1999) 1:, 190–192

17. Stein I., Itin, A., Einat, P., Skaliter, R., Grossman, Z. and Keshet, E. (1998) Translation of vascular endothelial growth factor mRNA by internal ribosome entry: implications for translation under hypoxia. Mol. Cell. Biol., 18:3112–3119

18. Fernandez J., Yaman, I., Mishra, R., Merrick, W.C., Snider, M.D., Lamers, W.H. and Hatzoglou, M. Internal ribosome entry site-mediated translation of a mammalian mRNA is regulated by amino acid availability. J. Biol. Chem. (2001) 276 :12285–1229

19. V. Zeenko and D.R. Gallie, Cap-independent translation of tobacco etch virus is conferred by an RNA pseudoknot in the 5'-leader, J Biol Chem (2005) 280:26813-24

20. D. Gallie, R. Tanguay and V. Leathers, The tobacco etch viral 5' leader and poly(A) tail are synergistic regulators of translation, Gene (1995) 165:233-238.

21. D.R. Gallie, Cap-independent translation conferred by the 5' leader of tobacco etch virus is eukaryotic initiation factor 4G dependent, J Virol (2001) 75:12141-52.

22. J.C. Carrington and D.D. Freed, Cap-independent enhancement of translation by a plant potyvirus 5' nontranslated region, J Virol (1990) 64:1590-7.

23. D.R. Gallie and K.S. Browning, eIF4G functionally differs from eIFiso4G in promoting internal initiation, cap-independent translation, and translation of structured mRNAs, J Biol Chem (2001) 276:36951-60.

24. S. Ray, H. Yumak, A. Domashevskiy, M.A. Khan, D.R. Gallie and D.J. Goss, Tobacco Etch Virus mRNA Preferentially Binds Wheat Germ Eukaryotic Initiation Factor (eIF) 4G Rather than eIFiso4G, J Biol Chem (2006) 281:35826-34.

25. Browning, K. S., Webster, C., Roberts, J. K., and Ravel, J. M. , Identification of an isozyme form of protein synthesis initiation factor 4F in plants. J Biol Chem (1992) 267: 10096-10100

26. Abramson, R. D., Browning, K. S., Dever, T. E., Lawson, T. G., Thach, R. E., Ravel, J. M., and Merrick, W. C. Initiation factors that bind mRNA. A comparison of mammalian factors with wheat germ factors J Biol Chem (1988) 263:5462-5467

27. Lax, S. R., Browning, K. S., Maia, D. M., and Ravel, J. M. ATPase activities of wheat germ initiation factors 4A, 4B, and 4F, J Biol Chem (1986) 261: 15632-15636

28. Browning, K. S., Lax, S. R., and Ravel, J. M, Identification of two messenger RNA cap binding proteins in wheat germ. Evidence that the 28-kDa subunit of eIF-4B and the 26-kDa subunit of eIF-4F are antigenically distinct polypeptides, J Biol Chem (1987) 262: 11228-11232

29. Humphreys J, Browning KS, Ravel JM. Identification of a Kinase in Wheat Germ that Phosphorylates the Large Subunit of Initiation Factor 4F , Plant Physiol. (1988): 88(2):483-486.

30. Gross JD, Matsuo H, Fletcher M, Sachs AB, Wagner G. Interactions of the eukaryotic translation initiation factor eIF4E. Cold Spring Harb Symp Quant Biol. (2001) 66:397-402. Review

31. Carberry, S. E., and Goss, D. J. Wheat germ initiation factors 4F and (iso)4F interact differently with oligoribonucleotide analogues of rabbit alpha-globin mRNA. Biochemistry (1991) 30: 4542-4545

32. Gallie, D. R., and Browning, K. S. eIF4G functionally differs from eIFiso4G in promoting internal initiation, cap-independent translation, and translation of structured mRNAs. J Biol Chem (2001) 276: 36951-36960

33. Gallie, D. R .Cap-independent translation conferred by the 5' leader of tobacco etch virus is eukaryotic initiation factor 4G dependent. J Virol (2001) 75:12141-12152

34. Rogers, G. W., Jr., Richter, N. J., and Merrick, W. C Biochemical and kinetic characterization of the RNA helicase activity of eukaryotic initiation factor 4A. J. Biol. Chem. (1999) 274: 12236–12244

35. Rogers, G. W., Jr., Richter, N. J., Lima, W. F., and Merrick, W. C. Modulation of the helicase activity of eIF4A by eIF4B, eIF4H, and eIF4F. J. Biol. Chem. (2001) 276: 30914–30922

36. Dever T.E. Translation initiation: adept at adapting. Trends Biochem. Sci. (1999) 24: 398–403.

37. Hernández G, Vazquez-Pianzola P. Functional diversity of the eukaryotic translation initiation factors belonging to eIF4 families. Mech Dev. (2005);122 (7-8):865-76.

38. Gallie, D. R .A tale of two termini: a functional interaction between the termini of an mRNA is a prerequisite for efficient translation initiation. Gene. (1998) 17;216(1):1-11.

39. Lax SR, Lauer SJ, Browning KS, Ravel JM. Purification and properties of protein synthesis initiation and elongation factors from wheat germ. Methods Enzymol. (1986) 118:109-28.

40. Shijun Cheng and Daniel R. Gallie Wheat eukaryotic initiation factor 4B organizes assembly of RNA and eIFiso4G, eIF4A, and poly(A)-binding protein. J. Biol. Chem., (2006) 281: 34, 24351-24364,

41. Luo, Y., and Goss, D. J. Homeostasis in mRNA initiation: wheat germ poly(A)-binding protein lowers the activation energy barrier to initiation complex formation.J. Biol. Chem. (2001) 276:43083–43086

42. Khan, M. A., and Goss, D. J. Translation initiation factor (eIF) 4B affects the rates of binding of the mRNA m7G cap analogue to wheat germ eIFiso4F and eIFiso4F.PABP. Biochemistry (2005) 44: 4510–4516

43. Trachsel, H., Erni, B., Schreier, M. H., and Staehelin, T. Initiation of mammalian protein synthesis. II. The assembly of the initiation complex with purified initiation factors. J. Mol. Biol. . (1977) 116, 755–767

44. Benne, R., and Hershey, J. W. The mechanism of action of protein synthesis initiation factors from rabbit reticulocytes. J. Biol. Chem. (1978) 253, 3078–3087

45. Pestova, T. V., Hellen, C. U., and Shatsky, I. N. Functional dissection of eukaryotic initiation factor 4F: the 4A subunit and the central domain of the 4G subunit are sufficient to mediate internal entry of 43S preinitiation complexes. Mol Cell Biol. (1996) 12:6870-8.

46. Le, H., Tanguay, R. L., Balasta, M. L., Wei, C.-C., Browning, K. S., Metz, A. M., Goss, D. J., and Gallie, D. R. Translation initiation factors eIF-iso4G and

eIF-4B interact with the poly(A)-binding protein and increase its RNA binding activity. J. Biol. Chem (1997) 272: 1624

47. Gallie, D. R., and Tanguay, R.Poly(A) binds to initiation factors and increases cap-dependent translation in vitro. . J. Biol. Chem. (1994) 269:17166–17173

48. Metz, A. M., Wong, K. C., Malmstrom, S. A., and Browning, K. S. Eukaryotic initiation factor 4B from wheat and Arabidopsis thaliana is a member of a multigene family. Biochem. Biophys. Res. Commun. (1999) 266, 314–321

49. Tarun, S. Z., Jr., and Sachs, A. B. Association of the yeast poly(A) tail binding protein with translation initiation factor eIF-4G. Embo J (1996) 15: 7168-7177

50. Wei, C.-C., Balasta, M. L., Ren, J., and Goss, D. J. Wheat germ poly(A) binding protein enhances the binding affinity of eukaryotic initiation factor 4F and (iso)4F for cap analogues. Biochemistry (1998) 37:1910-1916

51. L.J. Otero, M.P. Ashe and A.B. Sachs, The yeast poly(A)-binding protein Pab1p stimulates in vitro poly(A)-dependent and cap-dependent translation by distinct mechanisms. EMBO J. (1999) 18:3153–3163

52. S.A. Adam, T. Nakagawa, M.S. Swanson, T.K. Woodruff and G. Dreyfuss, mRNA polyadenylate-binding protein: gene isolation and sequencing and identification of a ribonucleoprotein consensus sequence. Mol. Cell. Biol. (1986) 6: 2932–2943.

53. A.B. Sachs, M.W. Bond and R.D. Kornberg, A single gene from yeast for both nuclear and cytoplasmic polyadenylate-binding proteins: domain structure and expression. Cell (1986) 45: 827–835.

54. U. Kühn and T. Pieler, Xenopus poly(A) binding protein: functional domains in RNA binding and protein–protein interaction. J. Mol. Biol. (1996) 256: 20–30.

55. C.G. Burd, E.L. Matunis and G. Dreyfuss, The multiple RNA-binding domains of the mRNA poly(A)-binding protein have different RNA-binding activities. Mol. Cell. Biol. (1991) 11:3419–3424.

56. H. Le, K.S. Browning and D.R. Gallie, The phosphorylation state of poly(A)-binding protein specifies its binding to poly(A) RNA and its interaction with eukaryotic initiation factor (eIF) 4F, eIFiso4F, and eIF4B, J Biol Chem (2000) 275: 17452-62.

57. Carpousis, A. J. The RNA degradosome of Escherichia coli: an mRNA-degrading machine assembled on RNase E .Annual Review of Microbiology (2007) 61(1): 71-87

58. J.J. Kohler and A. Schepartz, Kinetic studies of Fos.Jun.DNA complex formation: DNA binding prior to dimerization, Biochemistry (2001) 40:130-42.

59. M.A. Khan, H. Miyoshi, D.R. Gallie and D.J. Goss, Potyvirus genome-linked protein, VPg, directly affects wheat germ in vitro translation: interactions with translation initiation factors eIF4F and eIFiso4F, J Biol Chem (2008) 283: 1340-9.

60. Bi, X., and Goss, D. J. Wheat germ poly(A)-binding protein increases the ATPase and the RNA helicase activity of translation initiation factors eIF4A, eIF4B, and eIF-iso4F, J. Biol. Chem. (2000) 275: 17740-17746.

61. Michel YM, Poncet D, Piron M, Kean KM, Borman AM. Cap-Poly(A) synergy in mammalian cell-free extracts. Investigation of the requirements for poly(A)-mediated stimulation of translation initiation.J Biol Chem. (2000) 275 (41):32268-76.

62. T. Preiss and M.W. Hentze, Dual function of the messenger RNA cap structure in poly(A)-tail-promoted translation in yeast. Nature (1998) 392: 516–520.

63. A. Proweller and J.S. Butler, Ribosome concentration contributes to discrimination against poly(A)$^-$ mRNA during translation initiation in Saccharomyces cerevisiae. J. Biol. Chem. (1997) 272: 6004–6010.